Neutron-Deficient Members of the $A=139$ Decay Chain. I. 5.5-h Nd^{139m} and 30-min Nd^{139g}

D. B. BEERY* AND W. H. KELLY

Cyclotron Laboratory,† Department of Physics, Michigan State University, East Lansing, Michigan 48823

AND

WM. C. MCHARRIS

Department of Chemistry‡ and Cyclotron Laboratory,† Department of Physics, Michigan State University, East Lansing, Michigan 48823

(Received 17 March 1969)

We have studied the γ rays emitted following the decays of 5.5-h Nd^{139m} and 30-min Nd^{139g} with Ge(Li) and NaI(Tl) detectors in singles, coincidence, and anticoincidence configurations. Our study has indicated 51 γ rays accompanying Nd^{139m} decay and 21 that follow Nd^{139g} decay. Of these, 56 have been placed in decay schemes containing a total of 22 excited states. The decay scheme of $\frac{3}{2}+$ Nd^{139g} has much in parallel with those of similar nuclei in this region, and states are populated in Pr^{139} at 0 ($\frac{5}{2}+$), 113.8 ($\frac{7}{2}+$), 405.0 ($\frac{3}{2}+$, $\frac{1}{2}+$), 589.2 ($\frac{5}{2}+$), 916.8 ($\frac{1}{2}+$, $\frac{3}{2}+$), 1074.4 ($\frac{1}{2}+$, $\frac{3}{2}+$), 1311.8 ($\frac{1}{2}+$, $\frac{3}{2}+$, $\frac{5}{2}+$), 1328.2 ($\frac{5}{2}+$), 1405.5 ($\frac{1}{2}+$, $\frac{3}{2}+$, $\frac{5}{2}+$), 1449.5 ($\frac{1}{2}+$, $\frac{3}{2}+$, $\frac{5}{2}+$), and 1501.2 keV ($\frac{1}{2}+$, $\frac{3}{2}+$). On the other hand, 11/2− Nd^{139m} decays only 12.7% via a 231.2-keV $M4$ isomeric transition and independently decays by electron capture to a set of almost completely different states in Pr^{139}. These are at 0 ($\frac{5}{2}+$), 113.8 ($\frac{7}{2}+$), 821.9 (11/2−), 828.1 ($\frac{7}{2}+$, $\frac{9}{2}+$), 851.9 ($\frac{9}{2}+$, $\frac{7}{2}+$), 1024.0 ($\frac{7}{2}+$, $\frac{9}{2}+$, 11/2+), 1396.6 ($\frac{9}{2}$, 11/2, 13/2), 1523.2, 1624.5 ($\frac{9}{2}-$, 11/2−), 1834.1 ($\frac{9}{2}-$, 11/2−), 1927.1 ($\frac{9}{2}-$, 11/2−), 2048.8 ($\frac{9}{2}-$, 11/2−), 2174.3 ($\frac{9}{2}-$, 11/2−), and 2196.7 keV ($\frac{9}{2}-$, 11/2−). Some 80.7% of its decay goes to the last six states, and we interpret them as being *three-quasiparticle* states. It appears that Nd^{139m} is one of a few nuclides whose intrinsic structure forces the preferred mode of decay to go into a three-quasiparticle multiplet, i.e.,

$$(\pi d_{5/2})^2(\nu d_{3/2})^{-2}(\nu h_{11/2})^{-1}\rightarrow(\pi d_{5/2})(\nu d_{3/2})^{-1}(\nu h_{11/2})^{-1}.$$

The three-quasiparticle states are depopulated by numerous enhanced γ transitions between states in the multiplet and fewer, apparently highly hindered, transitions to lower states. Thus, the potential exists for extracting information about states near 2 MeV in this nucleus that normally is available only for states near the ground state.

I. INTRODUCTION

ONE of the most interesting regions of the nuclidic chart for current study is the region just below $N=82$, for here many systematic examples of rather extreme isomerism can be observed. The neutron-deficient side of the $A=139$ decay chain juts out into this region, and its members are well suited for probing the region because nuclei rather far removed from β stability are reached not too far below the closed shell. Thus, many interesting states should be populated by their decay, and these states should still be amenable to explanation in relatively straightforward shell-model terms—the number of nucleons making substantial contributions to a given configuration should not be so large as to be completely unmanageable.

$_{58}Ce_{81}^{139}$ is the first radioactive member on this side of the chain, and it decays directly to stable La^{139} with an electron-capture Q-value Q_ϵ of only 270 keV and a half-life of 140 days; it has a very simple decay scheme that has been known for a long time.[1] It does, however, have an interesting $h_{11/2}$ isomeric state (746 keV; $t_{1/2}=55$ sec), a member of the extensive $N=81$ series. The decay of the second radioactive member, 4.5-h $_{59}Pr_{80}^{139}$, to Ce^{139} is considerably more complex; we describe our results on this decay scheme in the following paper.[2]

$_{60}Nd_{79}^{139}$ is thrice removed from stable La^{139} and has a rather large amount of energy available for β decay ($Q_\epsilon=2.8$ MeV; cf. below). As in other $N=79$ odd-mass isotones, the $h_{11/2}$-$d_{3/2}$ (metastable-ground state) separation is fairly small, making the $M4$ isomeric transition quite slow. This means that here we are presented with two dissimilar isomers decaying almost independently, and because each can populate reasonably high-lying states in Pr^{139}, a wealth of information about many quite different states in this daughter nucleus is available from the study of these decays.

Nd^{139m} was first observed by Stover[3] in 1950 as part of an investigation of the products of bombardment of Pr^{141} with 40- and 50-MeV protons. Chemical identification was performed by ion exchange, and the mass number was established with reference to the granddaughter Ce^{139}. The half-life was measured to be 5.5±0.2 h.

---

* Present address: Manchester College, North Manchester, Ind. 46962.

† Work supported in part by the U. S. National Science Foundation.

‡ Work supported in part by the U. S. Atomic Energy Commission.

[1] M. L. Pool and N. L. Krisberg, Phys. Rev. **73**, 1035 (1958).

[2] D. B. Beery, W. H. Kelly, and Wm. C. McHarris, following paper, Phys. Rev. **188**, 1875 (1969).

[3] B. J. Stover, Phys. Rev. **81**, 8 (1951).

Later studies[4,5] of conversion electron intensities and energy differences for a 231-keV transition accompanying this decay indicated it to be an $M4$ and to originate in Nd not Pr. Four neighboring odd-mass isobars with 79 neutrons were known[6] to have isomeric states involving an $\frac{11}{2}-\rightarrow\frac{3}{2}+$ transition. From the trends in the isomeric level energies and in the reduced transition probablities, Gromov and his co-workers concluded that here we have a like pair of states[4] and that the 5.5-h activity was the $\frac{11}{2}-$ metastable state.

The $\frac{3}{2}+$ ground state was not seen so easily, and its half-life was only recently measured[7] to be 29.7 ± 0.5 min. For that experiment, it was produced by bombarding Pr^{141} with 30- and 33-MeV deuterons.

The only previous studies of Nd^{139m} decay[4,8] resulted in rather sketchy decay schemes containing serious disagreements. Because of this and the absence of any decay scheme for Nd^{139g}, we felt that this would make a good system for investigation. Our study has indicated the presence of 51 γ rays accompanying Nd^{139m} decay and 21 that follow Nd^{139g} decay. Of these γ rays, 56 have been placed in decay schemes containing a total of 22 excited states. Fourteen of these states have not been seen before.

The decay scheme of Nd^{139g} turns out to be unexceptional, having much in parallel with the decay scheme[9] of Nd^{141} and some other nuclei in this region below $N=82$. The low-spin states that it populates in Pr^{139} can be characterized reasonably well and follow expected systematics. On the other hand, the decay scheme of Nd^{139m} is anything but standard. This high-spin isomer decays only 12.7% by the 231.2-keV isomeric transition, the rest being by β^+ or electron capture (ϵ) to mostly high-spin high-lying states in Pr^{139}. Six of these, between 1624.5 and 2196.7 keV, are populated by decay that is less hindered ($\log ft$'s between 5.5 and 6.3) than the decay to an $h_{11/2}$ isomeric state at 821.9 keV in Pr^{139} ($\log ft=7.0$), which is almost certainly an *allowed* transition. This would seem to indicate that the transitions to these six states are also allowed, which would imply odd-parity states.

We interpret this as the configuration of Nd^{139m} being peculiarly suited for populating a multiplet of *three-quasiparticle* states. During the explanation we discuss the problem associated with multiple particle rearrangements in β and γ decay.

II. SOURCE PREPARATION

The 5.5-h Nd^{139m} activity was produced for most of our experiments by the relatively clean $(p, 3n)$ reaction on 100%-abundant Pr^{141}. Targets of 99.999% pure[10] Pr_2O_3 were bombarded typically for ≈1 h with ≈2 μA of 29-MeV protons from the Michigan State University sector-focused cyclotron. Sources were allowed to decay for about 5 h to let the 30-min Nd^{139g} produced by the bombardments reach transient equilibrium with Nd^{139m}. Experiments were then performed with the sources for approximately 20 h, until the Pr^{140} produced by the 3.3-day decay of Nd^{140} became a significant contaminant.

From crude excitation function studies of reactions following the bombardment of Pr^{141} with protons of various energies, we were able to distinguish the Nd^{139m+g} activities from weak-contaminant activities. Following each bombardment with 29-MeV protons, we were able to identify every contaminant peak observed in spectra recorded between 20 min and 40 h after the end of the bombardment. These weak contaminants, roughly in decreasing order of importance, were Pr^{140}, Pr^{139}, Ce^{139}, Nd^{141}, and Pr^{142}. It is significant that we did not produce any 22-min Nd^{138}, for its daughter, 2.1-h Pr^{138}, could prove a troublesome contaminant.

Nd^{139m} sources were also produced (somewhat serendipitously) following the bombardments of Nd^{142} with 36-MeV τ's (He^3 ions) and of Pr^{141} by 48- and 60-MeV τ's, all from the MSU cyclotron. These reactions were not so clean as the $(p, 3n)$ reaction on Pr^{141}, but they confirmed the relative intensities of the Nd^{139m} γ rays.

Most of our Nd^{139g} sources were produced by bombarding similar Pr_2O_3 tragets with 29-MeV protons for ≈45 sec. Experiments were carried out immediately upon concluding each of the bombardments, and the γ rays resulting specifically from Nd^{139g} decay were followed as their intensities dropped from their initial values to those when Nd^{139g} was in transient equilibrium with Nd^{139m}.

The relative intensities of all the Nd^{139g} γ rays we observed were confirmed by measurements of the activity produced by 48- and 60-MeV τ's on Pr^{141}. These reactions would produce Pm^{139}, which, were it a low-spin nucleus as anticipated, would populate Nd^{139g} by β decay much more strongly than Nd^{139m}. They did, in fact, yield Nd^{139g}/Nd^{139m} isomer ratios some 30 times as large as the $(p, 3n)$ reaction on Pr^{141}, but they yielded many more interfering short-lived activities as well.

III. EXPERIMENTAL RESULTS FOR Nd^{139m}

A. γ-Ray Singles Spectra

A 7-cm^3 five-sided coaxial Ge(Li) detector manufactured[11] in this laboratory was employed to determine

[4] K. Ya. Gromov, A. S. Danagulyan, A. T. Strigachev, and V. S. Shpinel', Izv. Akad. Nauk SSSR, Ser. Fiz. **27**, 1357 (1963).
[5] J. Gilat and W. J. Tretyl, University of California Lawrence Radiation Laboratory Report No. UCRL-17299, p. 20, 1967 (unpublished).
[6] C. M. Lederer, J. M. Hollander, and I. Perlman, in *Table of Isotopes* (John Wiley & Sons, New York, 1966), 6th ed.
[7] J. Lange, Kernforschungszentrum Karlsruhe Report No. KFK-519, p. 47, 1967 (unpublished); summarized in J. Lange, H. Münzel, and I. Leitl, Radiochimica Acta **8**, 123 (1967).
[8] K. Ya. Gromov, A. S. Danagulyan, L. N. Nikityuk, V. V. Murav'eva, A. A. Sorokin, M. Z. Shtal', and V. S. Shpinel', Zh. Eksperim. i. Teor. Fiz. **47**, 1644 (1964) [English Transl.: Soviet Phys.—JETP **20**, 1104 (1965)].
[9] D. B. Beery, W. H. Kelly, and Wm. C. McHarris, Phys. Rev. **171**, 1283 (1968).
[10] Obtained from Allied Chemical Corp., General Chemical Div., 800 Marion Ave., River Rouge, Mich. Targets of 99.9% Pr_2O_3 obtained from K & K Laboratories, Plainview, N. Y., were also used.
[11] This detector was manufactured by Dr. G. Berzins working with Dr. C. R. Gruhn, to both of whom we express our appreciation.

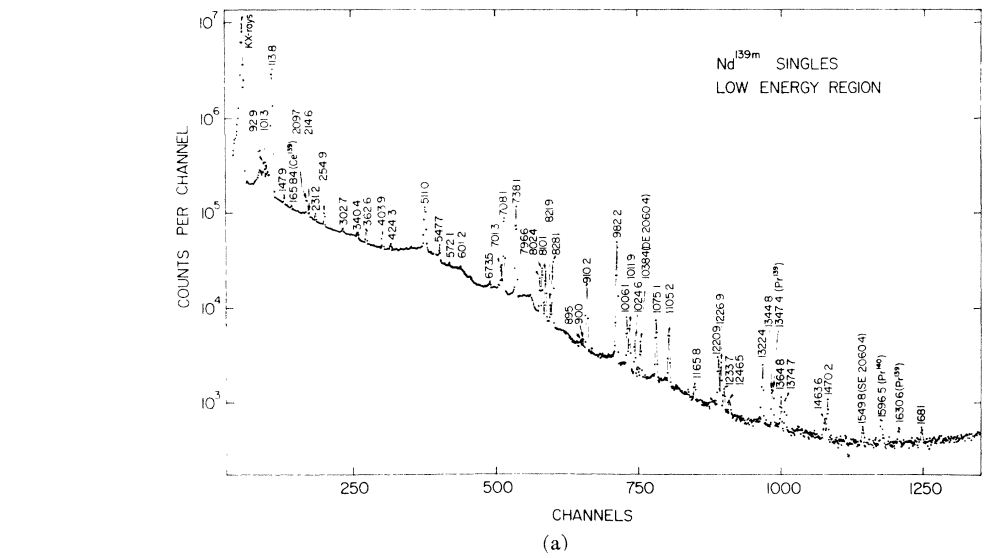

FIG. 1. (a) Nd^{139m} singles γ-ray spectrum taken with a 7-cm^3 Ge(Li) detector—low-energy portion. This spectrum was accumulated for a 1-day period, using multiple bombardments to obtain optimum sources. Because of analyzer spillover, the portion of the spectrum below ≈ 120 keV was recorded for a shorter period of time and then normalized to the remainder of the spectrum. (b) Nd^{139m} singles γ-ray spectrum taken with a 7-cm^3 Ge(Li) detector—high-energy portion. The events above 2300 keV come primarily from room background. From this spectrum an upper limit of 0.1% was placed on any transition with an energy greater than 2300 keV.

the energies and intensities of the Nd^{139m} γ rays. The wall thickness of the evacuated Al can enclosing the detector was 0.16 cm. Under typical operating conditions, a resolution of ≈ 2.5 keV full width at half-maximum (FWHM) for the 661.6-keV γ of Cs^{137} was obtained, using a room-temperature field-effect transistor (FET) preamplifier, a low-noise RC linear amplifier with pole-zero compensation, and a 4096-channel analyzer or analog-to-digital converter (ADC) coupled to a computer.

Energies of the prominent Nd^{139m} γ rays were measured by counting the Nd^{139m} sources simultaneously with several well-known calibration sources. To determine the energy calibration curve, we used a least-squares fit of the photopeak centroids of the calibration transitions to a quadratic equation after the background had been subtracted from under the peaks. The background correction for each peak was made by fitting a linear equation to several channels adjacent to both sides of the peak and then subtracting. The energies of the lower-intensity Nd^{139m} γ rays, which were obscured by the calibration standards, were then determined similarly by using the stronger Nd^{139m} γ rays as the standards. Some γ-ray singles spectra are shown in Figs. 1(a) and 1(b).

We used the spectrum shown in Fig. 1(b) to place an upper limit of 0.1% of the disintegrations of Nd^{139m} on any γ transition with an energy above 2300-keV. This would appear to rule out the 2350- and 2500-keV γ's proposed earlier[8,6] to have intensities ≈ 50 times as large as our upper limit. The events observed above 2300 keV in Fig. 1(b) come from long-lived room backgrounds that were not subtracted out.

The contaminant peaks seen in Fig. 1(a) accompany

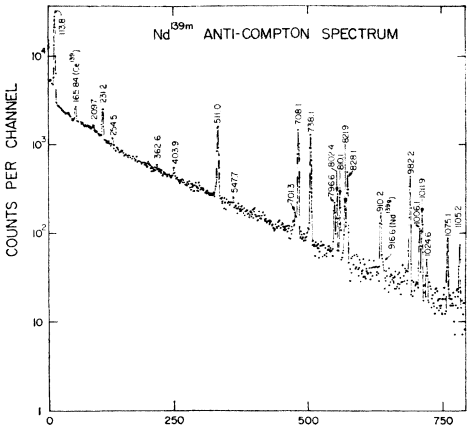

FIG. 2. Nd^{139m} anticoincidence spectrum recorded by the 7-cm³ Ge(Li) detector when placed inside the tunnel of an 8×8-in. NaI(Tl) split annulus, with a 3×3-in. NaI(Tl) detector at the other end of the tunnel. For details, see the text or Ref. 18. Characteristic of this type of spectrum is the noticeable absence of Compton edges. The 231.2-keV γ is the only γ ray enhanced over its singles intensity.

the reaction

$$Pr^{141}(p, 2n)Nd^{140} \xrightarrow{\epsilon} Pr^{140}$$

and Pr^{139} and Ce^{139} disintegrations following Nd^{139m+g} decay. Their energies, relative intensities, and intensity changes as functions of time were seen to be consistent with the properties of the associated decay schemes established in this study and elsewhere.[12–16,6]

A summary of the Nd^{139m} γ-ray energies and relative intensities is given in Table I. The energies assigned are mean values taken from a number of different measurements recorded at different times, different locations, with different system components, and with different parameters. Corresponding energy uncertainties are based on the reproducibilities of the Nd^{139m} energies from the calibration curves, the sizes of the Nd^{139m} photopeaks both before and after background subtraction, and the quoted errors on the standard energies.[17] The relative γ-ray intensities listed in Table I are also averages from a number of runs and were obtained using experimentally determined efficiency curves (cf. Ref. 9). Associated with these intensities are statistical uncertainties that include estimated uncertainties in the underlying backgrounds.

B. γ-γ Coincidence Studies

Coincidence and anticoincidence experiments were performed using Ge(Li)-NaI(Tl) spectrometers. For our first experiment, in order to determine which γ rays appear in cascades and which come primarily from ϵ-fed

TABLE I. Energies and relative intensities of γ rays present in the decay of Nd^{139m}.

Measured γ-ray energy (keV)	Relative intensity
92.9±0.2	3.2±0.6
101.3±0.8	0.7±0.2
113.8±0.1	133±25
147.9±0.1	2.5±0.5
209.7±0.1	6.2±0.6
214.6±0.2	1.4±0.4
231.2±0.2	2.4±0.2
254.9±0.3	3.7±0.6
302.7±0.3	1.4±0.2
340.4±0.5	2.7±0.5
362.6±0.2	6.2±0.5
403.9±0.3	8.0±1.0
424.3±0.3	2.0±0.4
511.0(γ±)	3.2±2.8[a]
547.7±0.3	7.5±0.7
572.1±0.5	1.7±0.4
601.2±0.8	1.3±0.4
673.5±0.5	2.5±0.7
701.3±0.3	13.0±2.0
708.1±0.1	72.0±2.0
733.0±1.0[b]	1.0±0.6[b]
738.1±0.2	≡100
796.6±0.3	13.0±2.0
802.4±0.3	21.0±2.0
810.1±0.3	18.0±2.0
821.9±0.3	3.7±0.4
828.1±0.2	29.0±2.0
851.9±0.5[b]	1.4±0.4[b]
895.1±0.6	0.8±0.2
900.3±0.6	1.1±0.3
910.2±0.2	21.6±2.0
982.2±0.2	79.0±2.0
1006.1±0.2	9.5±0.7
1011.9±0.2	8.0±0.6
1024.6±0.3	3.6±0.4
1075.1±0.2	9.6±1.0
1105.2±0.2	7.4±0.4
1165.8±0.5	1.0±0.5
1220.9±0.3	5.0±0.5
1226.9±0.3	4.0±0.4
1233.7±0.5	0.8±0.4
1246.5±1.0	0.9±0.4
1322.4±0.3	7.0±0.9
1344.8±0.6	1.3±0.4
1364.8±0.6	1.7±0.6
1374.7±0.5	1.8±0.5
1463.6±0.5	1.0±0.3
1470.2±0.3	2.0±0.5
1680.7±0.8	0.8±0.2
2060.4±0.2	15.5±1.0
2085.0±0.5	0.1±0.05
2201.2±0.8	0.3±0.1

[a] Calculated from the decay scheme proposed later in the present study. Components of the observed annihilation photon intensity from Nd^{139g} and/or Pr^{139} decay always exceed the Nd^{139m} component.

[b] Seen in coincidence spectra only. The intensities given here are inferred from the completed decay scheme and the behavior of these photons in the coincidence spectra.

[12] J. D. King, N. Neff, and H. W. Taylor, Nucl. Phys. **A99**, 433 (1967).

[13] D. De Frenne, J. Demuynck, K. Heyde, E. Jacobs, M. Dorikens, and L. Dorikens-Vanpraet, Nucl. Phys. **A106**, 350 (1968).

[14] K. Histake, Y. Yoshida, K. Etoh, and T. Murata, Nucl. Phys. **56**, 62 (19564).

[15] R. L. Graham and J. S. Geiger, Bull. Am. Phys. Soc. **11**, 11 (1966).

[16] H. W. Baer, J. J. Reidy, and M. L. Wiedenbeck, Nucl. Phys. **A113**, 33 (1968).

[17] The 59.543±0.015-keV calibration line from Am^{241} was included with the standards listed in Table I of Ref. 9 and in Table I in D. B. Beery, G. Berzins, W. B. Chaffee, W. H. Kelly, and Wm. C. McHarris, Nucl. Phys. **A123**, 681 (1969).

TABLE II. Relative intensities of photons in the decay of Nd^{139m} observed in coincidence experiments.

Energy (keV)	Relative intensity[a] Singles spectra	Anti-coincidence spectrum	113.8-keV γ-γ coinc. spectrum	113.8-keV γ-γ delayed coinc. spectrum	662-722 keV γ-γ coinc. spectrum	722-780 keV γ-γ coinc. spectrum
92.9	3.2	...	...	0.4	...	...
113.8	133.0	13	...	40	...	...
147.9	2.5	...	...	5	...	...
209.7	6.2	0.3	...	14	...	...
214.6	1.4	...	...	3	1.6	3.4
231.2	2.4	≡2.4[b]	...	<1.5	<1	<1
254.9	3.7	0.5	...	8.0	12	6.1
302.7	1.4	...	...	1.8	6.4	9.7
340.4	2.7	...	...	<0.6	<10	12
362.6	6.2	0.3	8	1.3	24	36
403.9	8.0	1.1	6	9.4	62	34
424.3	2.0	...	1	1.8	5.5	15
547.7	7.5	1.0	4	≡7.5	33	18
572.1	1.7	...	1	1.1	<4	16
601.2	1.3	...	2	<0.7	<6	<6
673.5	2.5	...	2	2.0	20	8
701.3	13	0.8	10	11	56	43
708.1	72	13	70	0.6	51	70
733	1.0	...	...	...	...	4
738.1	≡100	13	≡100	1.3	≡100	≡100
796.6	13	1.7	2	<1	18	48
802.4	21	2.3	14	18	98	60
810.1	18	2.4	17	<1	19	9.7
821.9	3.7	2.2	0.8	<1	<8	<8
828.1	29	5.7	3	0.9	35	103
851.9	1.4	0.4	...	<1	...	...
895.1	0.8	...	...	...	6	3
900.3	1.1	...	...	...	8	6
910.2	21.6	2.2	22	...	22	81
982.2	79	6.9	78	<1	285	461
1006.1	9.5	2.0	1	<1	11	40
1011.9	8.0	2.3	7	7.8	54	24
1024.6	3.6	0.5	4	<0.8	6.1	3
1075.1	9.6	1.8	9	<1	34	54
1105.2	7.4	1.4	4	6.6	43	27
1220.9	5.0	1.4	<1	<1	5.5	22
1226.9	4.0	0.6	2	4.7	21	12
1233.7	0.8	...	...	...	5	...
1322.4	7.0	1.6	5	<1	25	34
1344.8	1.3	...	0.8	<0.6	11	11
1364.8	1.7	...	1	0.9	10	6
1374.7	1.8	...	...	1.4	10	<8
2060.4	15.5	...	22	<5[d]	...	...
2085.0	0.1	...	0.2[c]	...	...	...

[a] All relative intensities from the coincidence runs are normalized with the aid of the singles spectra relative intensities listed here.

[b] This isomeric transition in Nd^{139} was the only transition seen which was not seen in coincidence with at least one other photon, thus it was used for normalization here.

[c] Only two counts observed.

[d] Limit placed on basis of absence of double escape peak and Compton background from the 2060.4-keV γ ray.

ground-state transitions, we employed an 8×8-in. NaI(Tl) split annulus detector in an anticoincidence experiment with the 7-cm^3 Ge(Li) detector.[18] The Nd^{139m} source was inserted into the center of the annulus tunnel, which was then blocked by a 3×3-in. NaI(Tl) detector at one end and by the Ge(Li) detector at the other end. By including the 3×3-in. NaI(Tl) detector in anticoincidence with the Ge(Li) detector, the Compton edges from backscattering in the Ge(Li) detector were reduced over what they would have been with only the annulus in anticoincidence. The single-channel analyzers associated with the NaI(Tl) detectors were set to accept all γ rays above 80 keV. A resolving time (2τ) of $\approx$100 nsec was used, and the true-to-chance ratio was usually $\approx$100/1. The resulting spectrum is shown in Fig. 2.

The 231.2- and 821.9-keV γ-ray peaks seen here were enhanced in the anticoincidence experiments (relative to their singles intensities) far more than were any of the other Nd^{139m} transitions, as indicated in Table II. Thus, each of the other Nd^{139m} γ rays appeared to be involved in one or more coincidences with $\gtrsim$80-keV photons. The following coincidence experiments elucidated most of these cascades.

A coincidence spectrum gated by the split annulus detector on the 113.8-keV γ is shown in Fig. 3. The γ-ray intensities seen in this experiment, normalized to

[18] R. L. Auble, D. B. Beery, G. Berzins, L. M. Beyer, R. C. Etherton, W. H. Kelly, and Wm. C. McHarris, Nucl. Instr. Methods **51**, 61 (1967).

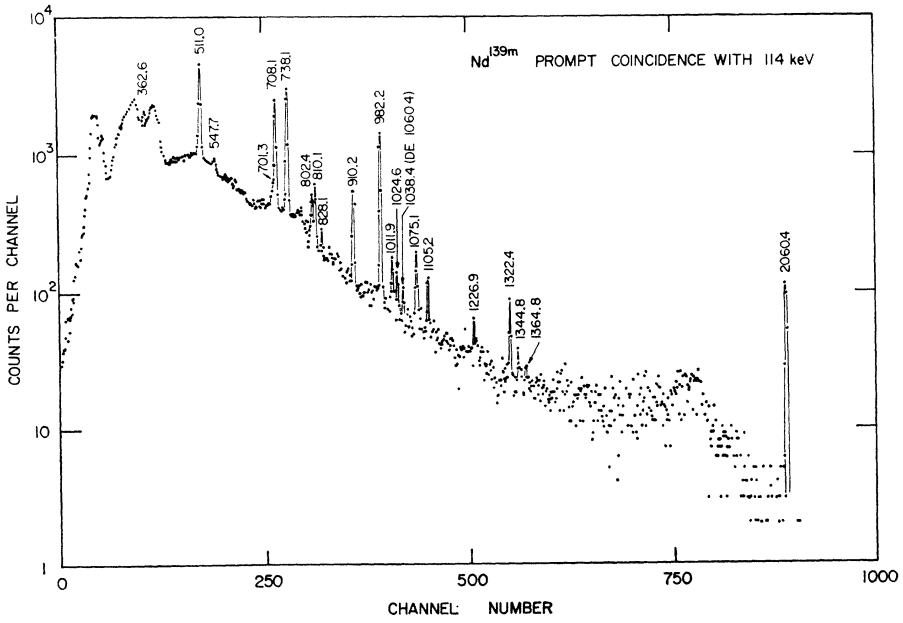

FIG. 3. Spectrum of Nd^{139m} γ rays in prompt coincidence with the 113.8-keV γ. The gate detector was the 8×8-in. NaI(Tl) split annulus, while the signal detector was the 7-cm³ Ge(Li) detector. The results are listed in Table III.

TABLE III. Summary of γ-γ anticoincidence and coincidence experiment results.

Gate interval[a] (keV)	γ in gate[b] (keV)	γ's enhanced[c] (keV)	Figure No.
Anticoincidence	≈80–2500	231.2, 821.9[e]	2
110–118	113.8[d]	362.6, 601.2, 708.1,[e] 810.1, 910.2, 982.2, 1024.6, 1038*DE*, 1075.1, 1322.4, 1344.8, 2060.4, 2085.0	3
110–118 Delayed display spectrum	113.8[d]	147.9, 209.7, 214.6, 254.9, 302.7, 403.9, 424.3, 547.7, 572.1, 673.5, 701.3, 802.5, 1011.9, 1105.2, 1226.9, 1364.8, 1374.7	6
400–408	403.9	701.3	f
500–600	511.0, *547.7*	362.6	f
450–550	*511.0*, 547.7	...	f
680–720	673.5, 701.3, *708.1*[e], 733, 738.1	254.9, 302.7, 403.9, 673.5, 701.3, 802.5, 895.1, 900.3, 1011.9, 1105.2, 1226.9, 1233.7, 1364.8, 1374.7	4
720–760	701.3, 708.1[e], 733, *738.1*	214.6, 340.4, 362.6, 733, 982.2, 1075.1, 1322.4	5
790–840	796.6, 802.4, *810.1*, 821.9[e] *828.1*, 851.9	209.7, 302.7, 424.3, 572.1 796.6, 828.1, 910.2, 1006.1, 1220.9	f
840–900	*828.1*, 851.9, 895.1, 900.3, *910.2*	601.2, 810.1, 1024.6, 1165.8	f
950–1150	*982.2*, 1006.1, 1011.9, 1024.6, 1075.1, 1105.2, 1165.8	214.6, 340.4, 362.6, 851.9	f
1180–1300	1165.8, *1220.9 1220.9*, 1233.7, 1246.5	821.9, 828.1	f
1900–2200	*2060.4*, 2085.0, 2201.2	113.8	f

[a] Prompt coincidence timing except where specified otherwise.

[b] Italicized γ energies carry the bulk of the γ intensity in the gates.

[c] That is, enhanced with respect to spectrum gated on adjacent regions. Conclusions summarized here are based on relative γ intensities in Table II, comparisons with results of other coincidence runs (to reduce gated background effects), and consideration of relative γ intensities within each run (to reduce effect of pulse heights on timing).

[d] Approximately $\frac{1}{3}$ of the population of the 113.8-keV state follows decay of the 821.9-keV state with a 40 nsec $t_{1/2}$.

[e] Delayed γ ray due to 40-nsec half-life of 821.9-keV state.

[f] These spectra can be seen in Ref. 19.

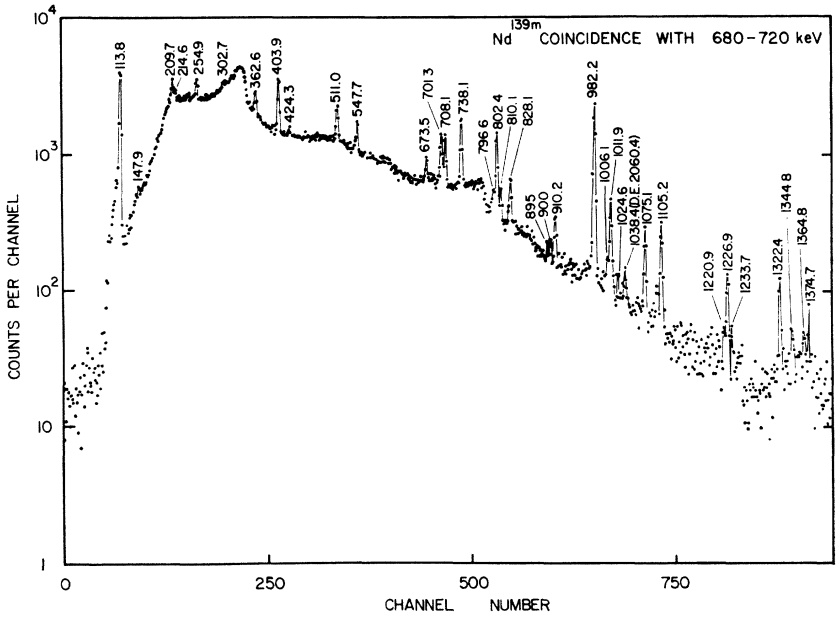

FIG. 4. Spectrum of Nd^{139m} γ rays in coincidence with the 680–720-keV energy interval. The gate signals came form the 8×8-in. NaI(Tl) split annulus.

100 for the 738.1-keV γ intensity, are listed in Table II. Here, four γ intensities are reduced by factors of about 10, viz., the 796.6-, 828.1-, 1006.1-, and 1220.9-keV γ's, whereas several other prominent peaks appear to be in coincidence with the intense 113.8-keV γ. These results are indicated in Table III.

In Figs. 4 and 5, we have the spectra resulting from gating this same spectrometer on two adjacent energy intervals, 680–720 and 720–760 keV. Because the resolution of the annulus in these experiments was only $\approx 13\%$, there was considerable overlap between these gated regions; however, as can be seen in Fig. 1(a) a single γ ray dominates each region, so a comparison of the intensities observed in coincidence with these adjacent gated regions was quite useful in constructing the decay scheme.

A comparison of the spectra recorded with adjacent coincidence gates also aided us in determining the effects of the underlying Compton backgrounds inevitably in the gates. In all we used 12 different gated

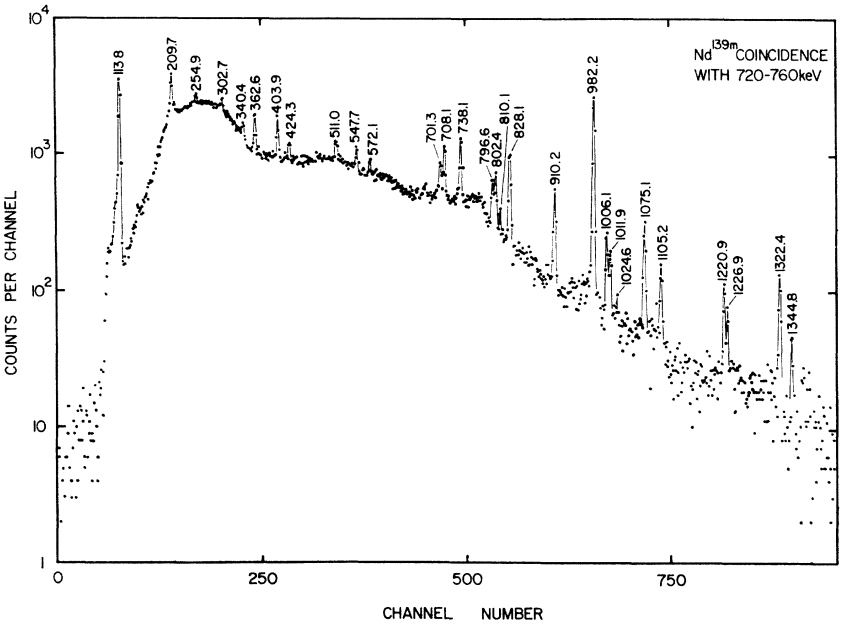

FIG. 5. Same as Fig. 4, except that the NaI(Tl) gate was set on the adjoining 720–760-keV energy interval.

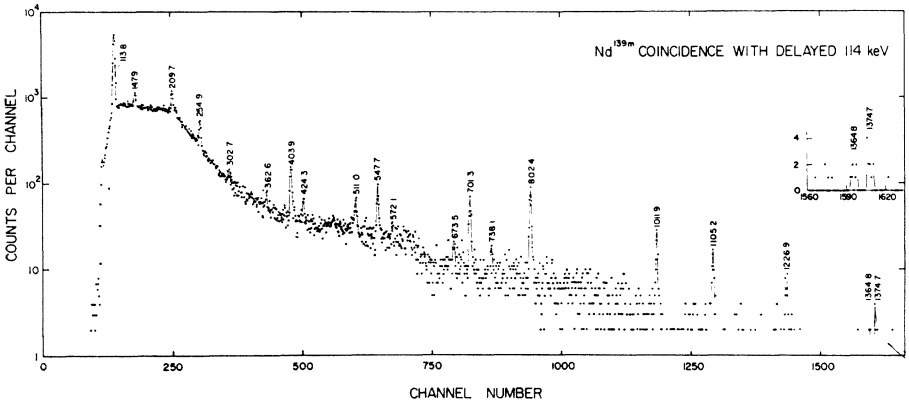

FIG. 6. Spectrum of Nd^{139m} γ rays in delayed coincidence with the 113.8-keV γ. A 3×3-in. NaI(Tl) scintillator was gated on the 113.8-keV γ and the timing resolution (2τ) of the coincidence circuit was $\approx$100 nsec, but a delay of $\approx$200 nsec was introduced into the Ge(Li) side of the circuit. Several peaks are enhanced by up to two orders of magnitude relative to the 708.1-, 738.1-, and 910.2-keV peaks, which were seen earlier to be in prompt coincidence with the 113.8-keV γ.

regions to obtain coincidence spectra[19] similar to those of Figs. 4 and 5. The results are summarized in Tables II and III.

C. Delayed Coincidence Experiments

It is possible that our single most useful coincidence experiment was a delayed coincidence experiment using a 3×3-in. scintillator and the Ge(Li) detector. The 3×3-in. NaI(Tl) scintillator was gated on the 113.8-keV γ, the coincidence timing resolution (2τ) was $\approx$100 nsec, and a delay of $\approx$200 nsec was added to the Ge(Li) side of the coincidence circuit. The resulting spectrum is shown in Fig. 6. Several peaks are enhanced up to 2 orders of magnitude relative to the 708.1-, 738.1-, and 910.2-keV peaks, which were seen earlier to be in prompt coincidence with the 113.8-keV γ. The intensities from this spectrum are listed in Table II. Later (Sec. IV A), we shall describe how this delayed coincidence spectrum confirms the placement of nine states in Pr^{139}.

The state responsible for the delays lies at 821.9 keV, and in order to measure its half-life, we used a fast-slow coincidence system with two 2×2-in. NaI(Tl) detectors and a time-to-amplitude converter (TAC). Now, from our prompt and delayed coincidence data we had no evidence for delays connected with states other than the 821.9-keV state. For this reason and because of leading-edge walk problems with lower-energy γ rays, we triggered the system with (prompt and delayed) pulses above 600 keV. The timing was chosen so that the prompt coincidence peak would be centered in the 512-channel analyzer used.

The time spectrum that remained following subtraction of the 17-counts/channel background is shown in Fig. 7. The resolution of the system was 3.3-nsec FWHM, and the timing calibration was made by inserting precisely measured pieces of delay cable into the circuit. No difficulties connected with channel widths or nonlinearities in the TAC were noted, so no corrections were made for these. The half-life calculated following a

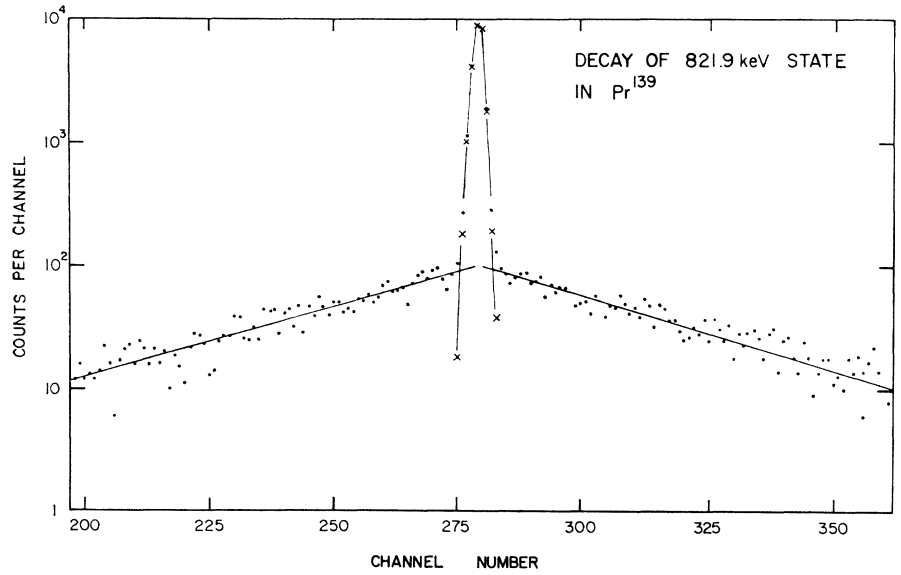

FIG. 7. Time-to-amplitude converter decay curve for the 821.9-keV state in Pr^{139}. The circuit used was symmetrical, with identical 2×2-in. NaI(Tl) detectors (gated on all pulses above 600 keV) starting and stopping a TAC. The calibration is 1.55 keV/channel, and the measured $t_{1/2}$ of the state is 40±2 nsec. Subtraction of the least-squared straight-line fit to the points produces the points indicated by x's, which show the resolution of the system to be 3.3-nsec FWHM.

[19] These are displayed in D. B. Beery, Ph.D. thesis, Michigan State University, 1969 (unpublished).

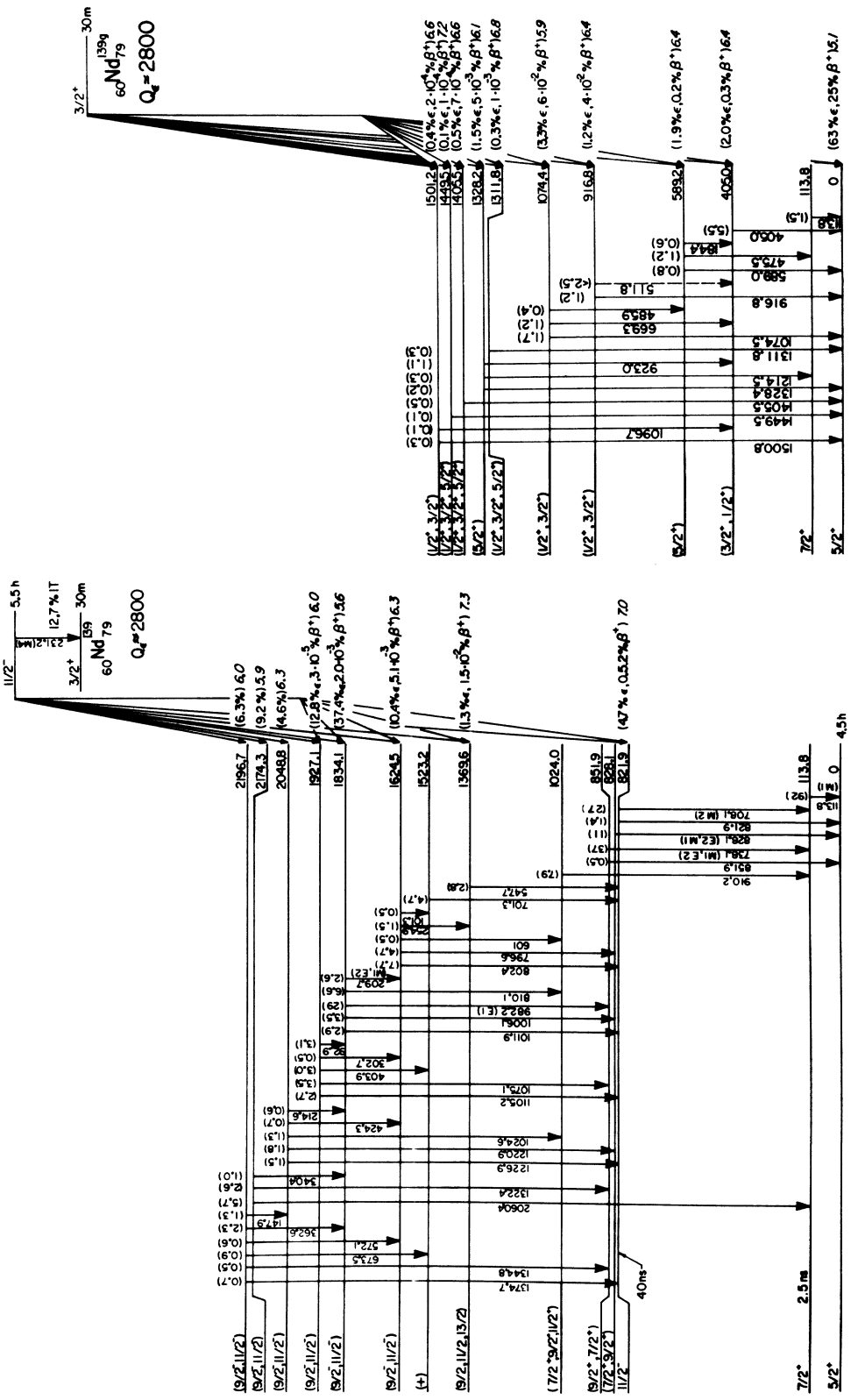

FIG. 8. Decay schemes of Nd^{139m} and Nd^{139g}. All energies are given in keV and (total) transition intensities are given in percent of the respective parent. The β^+/ϵ ratios are calculated values and the log ft values (in italics on the right-hand sides of the levels) are calculated on the basis of 5.5-h and 30-min half-lives.

TABLE IV. Cascade energy relations for Nd^{139m} γ rays.

γ rays in sum	Sum	State energy adopted
821.9	821.9	821.9
113.8+708.1	821.9	
851.9	851.9	851.9
113.8+738.1	851.9	
802.4+821.9	1624.3	1624.5
796.6+828.1	1624.7	
601+910.2+113.8	1625	
254.9+547.7+821.9	1624.5	
101.3+701.3+821.9	1624.5	
1011.9+821.9	1833.8	1834.1
1006.1+828.1	1834.2	
982.2+851.9	1834.1	
810.1+910.2+113.8	1834.1	
209.7+802.4+821.9	1834.0	
1105.2+821.9	1927.1	1927.1
1075.1+851.9	1927.0	
403.9+701.3+821.9	1927.1	
302.7+(1624.5 state)	1927.2	
92.9+(1834.1 state)	1927.0	
1226.9+821.9	2048.8	2048.8
1220.9+828.1	2049.0	
1024.6+910.2+113.8	2048.6	
424.3+(1624.5 state)	2048.8	
214.6+(1834.1 state)	2048.7	
2060.4+113.8	2174.2	2174.3
1322.4+851.9	2174.3	
340.4+(1834.1 state)	2174.5	
1374.7+821.9	2196.6	2196.7
1344.8+851.9	2196.7	
673.5+701.3+821.9	2196.7	
572.1+(1624.5 state)	2196.6	
362.6+(1834.1 state)	2196.7	
147.9+(2048.8 state)	2196.7	

least-squares fit of a straight line to the logarithms of the data in Fig. 7 was 40±2 nsec. No evidence of decays with different half-lives was observed in this experiment. The ratio of the areas under the prompt peak and the delayed curves are consistent with our decay scheme and our interpretation that the 821.9-keV state decays with a 40-nsec half-life.

IV. Nd^{139m} DECAY SCHEME

We have constructed a decay scheme for Nd^{139m} from the results of our coincidence studies and the energy sums and relative intensities of the transitions. This decay scheme is shown in Fig. 8, together with the decay scheme for Nd^{139g}, which we shall discuss later. The striking difference between the two decay schemes is worthy of note with the 113.8-keV γ being the only common transition. All energies are given in keV, and the Q_ϵ is a calculated value.[20] Total transition intensities are given in units of percent per disintegration of the parent Nd ^{39m} parent. The β^+/ϵ ratios are also calculated values using the method of Zweifel.[21] In general, the energy sums of competing crossover and cascade transitions agree to within ±0.2 keV. Because there are so many coincident, cascading transitions in this nucleus, there are many checks as to the energies of most of the levels. The energy assigned for each level is therefore a weighted value based both on the transitions that feed into and out of that level. Both because there are an abnormally large number of γ-ray branchings in this nucleus and because our interpretation of the higher-lying states makes it essential that they be convincingly placed, we have presented the relevant sets of sums in Table IV, where it can be seen that the self-consistency is excellent.

A. 113.8-keV Level and Those That Are Depopulated through It

The large relative intensity of the 113.8-keV γ combined with its coincidence behavior lead us to place a first-excited state at 113.8 keV, in agreement with earlier studies.[8,5]

The isomeric state at 821.9 keV was first placed on the basis of several prompt-coincidence experiments having timing resolutions (2τ) of $\approx$100 nsec (see, e.g., Table III). It was then confirmed by the delayed coincidence experiment of Fig. 6, which suggested that seven levels above 821.9 keV are depopulated through the 821.9-keV state. The γ transitions presumed to originate from these levels were enhanced by roughly two orders of magnitude over their intensities in prompt coincidence experiments (cf. Table II), and the ratio of each intensity to that of, say, the 547.7-keV γ is within $\approx$20% of what it was in the singles spectra. Not only were the direct transitions from these levels to the 821.9-keV state enhanced, but so were a myriad of interconnecting transitions. (At γ-ray energies below 300 keV, quantitative comparisons of the delayed γ-ray intensities with our decay scheme were significantly less precise because the earlier crossovers of the lower-energy pulses artificially introduced enhancement factors of >2 into the delayed coincidence spectrum.) The energies of these seven Pr^{139} states, at 1369.6, 1523.2, 1624.5, 1834.1, 1927.1, 2048.8, and 2196.7 keV, were assigned from the weighted energy sums listed in Table IV.

B. 828.1-, 851.9-, 1024.0-, and 2174.3-keV States

These four states are suggested by energy sums and relative γ-ray intensities (cf. Table I), as well as by the prompt coincidence data (Tables II and III). The absence from Fig. 6 of all ten of the γ rays indicated in our decay scheme to feed the 828.1-, 851.9-, and 1024.0-keV states is consistent with our interpretation of the positions of these states.

The 828.1-keV state is also confirmed by the suppression of the 796.6-, 828.1-, 1006.1, and 1220.9-keV γ's in the prompt coincidence experiments gated on the 113.8-keV γ (see Fig. 3 and Table II).

C. Remaining γ Rays

The 12 very weak γ rays observed at 733, 895.1, 900.3 1165.8, 1233.7, 1249.9, 1364.8, 1463.6, 1470.2, 1681,

[20] J. H. E. Mattauch, W. Thiele, and A. H. Wapstra, Nucl. Phys. **67**, 1 (1965); **67**, 32 (1965); **67**, 73 (1965).
[21] P. F. Zweifel, Phys. Rev. **107**, 329 (1957).

TABLE V. Multipolarity of γ transitions.

Transition energy[a] (keV)	K-electron intensity[b]	γ-ray intensity[c]	Experimental α_K	Theoretical α_K				Multipolarity
				$E1$	$E2$	$E1$	$E3$	
209.7	25±14	6.2±0.6	9.7(−2)	3(−2)	1.2(−1)	1.3(−1)	4.6(−1)	$M1, E2$
						$M3$	$M4$	
231.2	≡1000	2.4±0.2	≡9.5[d]	...	...	2.4	9.5	$M4$[e]
				$E3$	$M2$	$E4$	$M3$	
708.1	152±8	72±2	≡1.74(−2)[d]	9.5(−3)	1.74(−2)	2.0(−2)	4.1(−2)	$M2$[e]
				$E1$	$E2$	$M1$	$E3$	
738.1	≈50±7	≡100	4(−3)	1.4(−3)	3.6(−3)	5.6(−3)	8.1(−3)	$M1, E2$
				$E1$	$E2$	$M1$	$E3$	
828.1	10±3	29±2	3(−3)	1.2(−3)	2.8(−3)	4.4(−3)	6.3(−3)	$E2, M1$
				$E1$	$E2$	$M1$	$E3$	
982.2	8±2	79±2	8(−4)	8.3(−4)	2.0(−3)	2.9(−3)	4.2(−3)	$E1$

[a] Energies from present study.
[b] Relative K-electron intensities from Ref. 8.
[c] Relative γ-ray intensities from present work.
[d] The theoretical value of Ref. 23 was used, as Ref. 4 and Ref. 8 agreed on a multipolarity for this transition based on measured K/L electron intensity ratios.
[e] See Refs. 4 and 8 for descriptions of two independent measurements of this multipolarity.

2085.0, and 2201.2 keV have not been definitely placed in the level scheme. These γ rays do not fit between any existing states and do not significantly change the interpretation of the level scheme or its comparison with other nuclei or with theoretical calculations. The sum of these γ-ray intensities amounts to only 1.5% of the observed Nd^{139m} γ-ray intensity. Some tentatively suggested placements follow.

The 733-keV γ was seen only in coincidence with the 738.1-keV γ. The energies of these two sum to 1471.2 keV, within the measured uncertainty of the 1470.2-keV γ, thus tentatively suggesting a level at 1584.0 keV.

Evidence involving poor statistics indicates that the 2085.0-keV γ is in coincidence with the 113.8-keV γ, whereas the 2201.2-keV γ is not. On these grounds alone, tentative states at 2198.8 and 2201.2 keV may be inferred.

In order to obtain a lower limit for the logft values of transitions to these "unplaced" states, we assumed that each unplaced state was fed directly by ϵ decay and deexcites entirely by the unplaced γ rays. It then followed that the corresponding logft values would all be larger than about 7.8.

The properties of a few of the remaining five very weak γ rays (1165.8, 1233.7, 1249.9, 1463.6, and 1681 keV) can be seen in Table II. We are not able to find a unique location from them in our decay scheme. The sum of their intensity is less than 0.7% of the total observed Nd^{139m} γ rays.

V. SPIN AND PARITY ASSIGNMENTS FROM Nd^{139m} DECAY

A. Electron Data and Multipolarities

We compared our γ intensities with the conversion-electron intensity data of Gromov *et al.*[8,22] in order to gain multipolarity information about some of the more-intense lower-energy transitions following Nd^{139m} decay. These comparisons and predicted multipolarities are listed in Table V and plotted in Fig. 9. We were not able to use the conclusions of Gromov *et al.* directly because their γ intensities were obtained with NaI(Tl) scintillators and differ markedly from our data. However, from K/L conversion intensity ratios, the 231.2- and 708.1-keV transitions have been established to be $M4$ and $M2$, respectively, by both sets of previous workers.[8,5] The theoretical conversion coefficients[23] for these transitions were then used as a basis for determining the remaining coefficients. At lower energies ($\lesssim$300 keV) it appeared that the coefficients were affected by absorption in the electron-counter window.

B. Ground and Metastable States of Nd^{139}

Here, at $N=79$, one ought to consider three-quasiparticle (hole) states, but to a reasonable first approximation the low-lying ones can be thought of as single-hole states, so there are some similarities with the $N=81$ nuclides. Among the latter, there are now seven known that have $d_{3/2}$ ground states and $h_{11/2}$ isomeric states connected by $M4$ isomeric transitions.[24] Also, the $N=79$ nuclei Te^{131}, Xe^{133}, Ba^{135}, and Ce^{137} (Refs. 25–28, respectively) have $\frac{3}{2}+$ ground states and $\frac{11}{2}-$ meta-

[22] K. Gromov, V. Kalinnikov, V. Kuznetsov, N. Lebedev, G. Musiol, E. Herrmann, Zh. Zhelev, B. Dzhelepov, and A. Kudryavtseva, Nucl. Phys. **73**, 65 (1965).

[23] L. A. Sliv and I. M. Band, in *Alpha-, Beta-, and Gamma-Ray Spectroscopy*, edited by K. Siegbahn (North-Holland Publishing Co., Amsterdam, 1965).

[24] R. E. Eppley, Wm. C. McHarris, D. B. Beery, and W. H. Kelly, The New Isomer Gd^{145m} and the $N=81$ $M4$ Transition Probabilities (to be published).

[25] L. M. Beyer, G. Berzins, and W. H. Kelly, Nucl. Phys. **A93**, 436 (1967); W. B. Walters, C. E. Bemis, and G. E. Gordon, Phys. Rev. **140**, B268 (1965).

[26] J. M. Ferguson, D. L. Love, and D. Sam, J. Inorg, Nucl. Chem. **24**, 1 (1962).

[27] S. Morinobu, T. Hirose, and K. Hisatake, Nucl. Phys. **61**, 613 (1965).

[28] R. B. Frankel, Ph.D. thesis, University of California, Berkeley, Lawrence Radiation Laboratory Report No. UCRL-11871, 1964 (unpublished); D. B. Beery, W. H. Kelly, and Wm. C. McHarris (to be published).

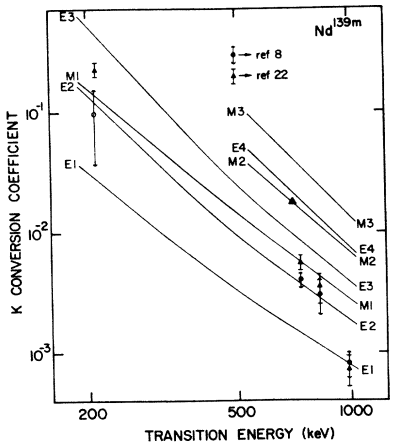

FIG. 9. A comparison of experimental and theoretical K-conversion coefficients for some of the γ transitions following Nd^{139m} decay. The lines are the theoretical values of Sliv and Band in Ref. 23. The data points were obtained by comparing the electron intensities of Gromov *et al.* (see Refs. 8, 22) with our γ-ray intensities, assuming the theoretical values of the 231.2- ($M4$) and 708.1-keV ($M2$) transitions to be correct for purposes of normalization.

stable states. Thus, when K-L conversion electron energy differences suggested that the 231.2-keV transition occurs in Nd rather than in Pr and the conversion line intensity confirmed that the transition was an $M4$, this indicated a similar $d_{3/2}$-$h_{11/2}$ isomer pair. We have plotted the energies of the $N=79$ and $N=81$ isomers in Fig. 10, including Nd^{139m} and a projection for Sm^{141m}.[29]

It is instructive to compare the reduced transition probability of the 231.2-keV γ with those of the other $M4$ γ rays, for these isomeric transitions should be among the best examples of true single-particle transitions. In Fig. 10, we have also plotted the squares of the radial matrix elements, $|M|^2$, of these transitions. These were calculated using Moszkowski's approximations for single-neutron transitions[30]

$$T_{SP}^{(ML)}=\frac{0.19(L+1)}{[(2L+1)!!]^2}|M|^2\left(\frac{\hbar\omega}{197\text{ MeV}}\right)^{2L+1}\times[a\text{ in }10^{-13}\text{ cm}]^{2L-1}\times S(j_i,L,j_f)\times 10^{21}\text{ sec}^{-1}.$$

Here, $T_{SP}^{(ML)}$ is the single-particle transition probability, L ($=4$ for $M4$'s) is the multipolarity, a ($=1.2\times 10^{-13}$ cm) is the effective nuclear radius, and $S(j_i, L, j_f)$ is a statistical factor (i.e., angular-momentum portion of the matrix element), which for $\frac{11}{2}\rightarrow\frac{3}{2}$ transitions has the value $\frac{15}{11}$.

The resulting values we obtained are consistently smaller than the approximation of a constant wave function,

$$|M|^2=[3/(L+2)]^2(\mu_n L)^2=14.6,$$

where μ_n is the magnetic moment of the neutron. This fact should not concern us, for $M4$ transitions are normally retarded over such estimates and one needs much more detailed information about the nuclear wave functions in order to make detailed comparisons meaningful. What is of more importance is the fact that the values of $|M|^2$ are not constant but show a definite trend in both the $N=79$ and $N=81$ nuclei. (It is unusual for $|M|^2$ not to be constant over such a series. For example, in the odd-mass neutron-deficient lead isotopes, $|M|^2$ was constant to the point that an apparent 15% discrepancy at Pb^{203} suggested that an unobserved transition was competing with the $M4$ isomeric transition. This competing transition was later discovered.[31])

Both because collective modes of the core would not be expected to contribute appreciably to a hexadecapole field and because the $h_{11/2}$ states cannot be mixed readily with other states in these nuclei, these $M4$ transitions should prove a more sensitive test of, say, $d_{5/2}$ and perhaps $s_{1/2}$ admixtures in the $d_{3/2}$ states than would normally be possible from electromagnetic transition rates. The fact that the $|M|^2$ values for the $N=79$ nuclei are consistently larger than those for the $N=81$ nuclei goes along with this, for the $N=79$ three-quasiparticle states would be expected to be much less pure, and only to a (good) first approximation can the transitions be characterized as proceeding from a pure $[(d_{3/2})^2h_{11/2}]_{11/2-}$ to a pure $[(d_{3/2})^3]_{3/2+}$ configuration. A more complete analysis of these $M4$ transitions, using the occupation number formalism, is presently underway.[24]

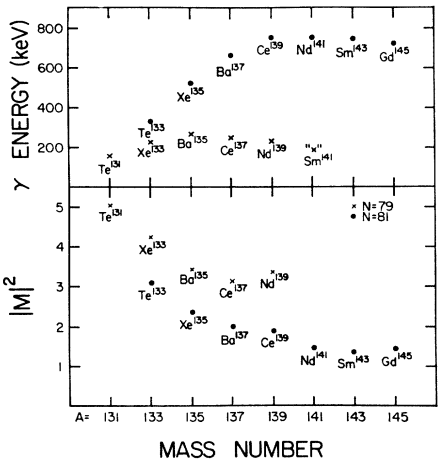

FIG. 10. Upper: Energies of the metastable states in the $N=79$ and $N=81$ isotones. (The Sm^{141} point is a predicted one.) Lower: Values of the squared radial matrix elements for the isomeric transitions in the same nuclei.

[29] R. Todd, R. E. Eppley, D. B. Beery, W. H. Kelly, and Wm. C. McHarris (unpublished).

[30] S. A. Moszkowski, in *Alpha-, Beta-, and Gamma-Ray Spectroscopy*, edited by K. Siegbahn (North-Holland Publishing Co., Amsterdam, 1965); S. A. Moszkowski, Phys. Rev. **89**, 474 (1953).

[31] R. E. Doebler, Wm. C. McHarris, and C. R. Gruhn, Nucl. Phys. **A120**, 489 (1968).

C. Ground, 113.8-, and 821.9-keV States in Pr^{139}

The ground state of Pr^{139} is fed by the $d_{3/2}$ ground state of Nd^{139}. In our study of this decay (see below, Secs. VI, VII) we obtained a logft value of 5.1 for this transition, which suggests $\frac{1}{2}+$, $\frac{3}{2}+$, or $\frac{5}{2}+$ for the ground state of Pr^{139}. Any of these assignments could be consistent with the observed[2] 99% of Pr^{139} β-decay (log$ft=5.3$) to the $\frac{3}{2}$ ground state of Ce^{139}. The simple shell-model predictions by Kisslinger and Sorensen,[32] and systematics of odd-mass nuclei with odd proton numbers between 51 and 63 indicate $\frac{5}{2}+$ and $\frac{7}{2}+$ configurations for the two lowest levels of Pr^{139}. Sixteen nuclei in this region have ground state and first excited states well characterized,[6] and in every case the assignments are $\frac{5}{2}+$ and $\frac{7}{2}+$ or $\frac{7}{2}+$ and $\frac{5}{2}+$.

The measured K and L conversion electron intensities for the 113.8-keV transition and its 2.5-nsec half-life[33] are characteristic of the l-forbidden $M1$ transitions between $g_{7/2}$ and $d_{5/2}$ states. Sixteen of these also have been measured[6] in odd-proton nuclei between $Z=51$ and $Z=63$.

No direct β-population of the 113.8-keV state was observed from either the $\frac{3}{2}+$ or $\frac{11}{2}-$ states of Nd^{139}. This is consistent with a $\frac{7}{2}+$ assignment for this state. Our upper limit of 3% ϵ decay to it from Nd^{139m} places a lower limit for the logft at 7.6, although we really expect the logft to be appreciably higher. The ϵ decay from some of the $h_{11/2}$ Te and Sn isomers to $g_{7/2}$ states in their daughter nuclei has been observed,[34] and the logft's cluster around 9. For an estimated log$ft=9$ for decay to the 113.8-keV state in Pr^{139}, the corresponding ϵ decay is only 0.1%.

The above cumulative evidence rather strongly suggests $\frac{5}{2}+$ and $\frac{7}{2}+$ assignments for the ground and first excited states in Pr^{139}, which would imply $d_{5/2}$ and $(g_{7/2})^{-1}(d_{5/2})^2$ configurations.

The measured α_K (Table V) of the 708.1-keV transition indicated it to be an $M2$, and this, combined with our evidence of direct feeding of the 821.9-keV state by Nd^{139m}, suggests this state to be $\frac{11}{2}-$. Our measured 40-nsec $t_{1/2}$ is consistent with this assignment. We have not determined the amounts of admixing in the γ transitions, but Weisskopf single-particle estimates[35] for the $t_{1/2}$'s of a 708.1-keV pure $M2$ and an 821.9-keV pure $E3$ are 1.2×10^{-9} and 1.3×10^{-6} sec, respectively. Thus, the $M2$ (partial $t_{1/2}=42$ nsec) appears to be retarded over the single-particle estimate. This is not particularly surprising, however, as $M2$'s are customarily retarded. More interesting, the $E3$ (partial $t_{1/2}=600$ nsec) appears to be *enhanced* over the single-particle estimate, and $E3$'s also are most often retarded.[36] However, there are three other known enhanced $E3$'s, in La^{137}, Eu^{147}, and Eu^{149} (Refs. 37 and 38), all just below or above the $N=82$ shell. More will be said about this in Sec. IX in terms of possible octupole admixtures in the 821.9-keV state, but the dominant characteristics of this state warrant the assignment $h_{11/2}$. The logft of 7.0 for the ϵ population of this state is high but certainly within the realm of possibilities for an $\frac{11}{2}-\longrightarrow\frac{11}{2}-$ allowed transition. We shall see later (Sec. IX) that the reason for this is that a multiparticle rearrangement is necessary for Nd^{139m} to populate this state.

D. 828.1-, 851.9-, and 1024.0-keV States

The 828.1-keV γ appears to be of $E2$ and/or $M1$ multipolarity, which sets limits of $\frac{1}{2}+$ through $\frac{9}{2}+$ on the 828.1-keV state. This state is fed strongly by the 1624.5-, 1834.1-, and 2048.8-keV states, each of which is populated directly by $\frac{11}{2}-$ Nd^{139m}, so $\frac{1}{2}+$, $\frac{3}{2}+$, and possibly $\frac{5}{2}+$ can probably be eliminated. If the state were $\frac{9}{2}+$, one might expect some direct ϵ feeding (first forbidden); we see none, but our limits are not too precise on this—we mention it in anticipation of the problems that will arise concerning some of the higher-lying states. A $\frac{9}{2}+$ assignment would also suggest that the 828.1-keV transition be pure $E2$, but again the precision in α_K does not allow one to say concretely whether this transition does or does not contain some $M1$ character. We can place an upper limit of 0.27% (of Nd^{139m} disintegrations) on the missing 714.3-keV γ to the $\frac{7}{2}+$ 113.8-keV state. The absence of this transition is slightly surprising, considering either a $\frac{7}{2}+$ or $\frac{9}{2}+$ assignment, but, for example, a core-coupled configuration involving the $d_{5/2}$ ground state could result in either but would explain the absence of such a transition. We are left with both $\frac{7}{2}+$ and $\frac{9}{2}+$ as possible assignments.

Using the same approach with the 851.9-keV state, we obtain $\frac{9}{2}+$ as the probable assignment, with $\frac{7}{2}+$ as a somewhat less likely alternative. Again, the 738.1-keV γ appears to be $M1$ and/or $E2$, which sets limits of $\frac{3}{2}+$ through $\frac{11}{2}+$ for the state. This state is fed strongly by the 1834.1-, 1927.1-, 2174.3−, and 2196.7-keV states, each of which is populated directly by what looks like an allowed transition. In particular, the intense 982.2-keV γ from the 1834.1-keV state—the state with the strongest claim to being a high-spin $(\frac{9}{2},\frac{11}{2})$ odd-parity state—is characterized as an $E1$. This permits us to narrow the assignments down to $\frac{7}{2}+$, $\frac{9}{2}+$, and $\frac{11}{2}+$. $\frac{11}{2}+$ can be ruled out on the basis of the branching ratio of the 738.1- and 851.9-keV γ's, for it would force the 851.9-keV γ to be an $M3$, which has a predicted (single-particle estimate) $t_{1/2}$ of 1.0×10^{-6} sec, as compared with only 2.7×10^{-11} sec for a 738.1-keV $E2$. The

[32] L. S. Kisslinger and R. A. Sorensen, Kgl. Danske Videnskab. Selskab, Mat.-Fys. Medd. **32**, No. 9 (1960).
[33] A. A. Sorokin, Zh. Eksperim. i. Teor. Fiz. **47**, 1232 (1964) [English transl.: Soviet Phys.—JETP **20**, 833 (1965)].
[34] G. Berzins and W. H. Kelly, Nucl. Phys. **A92**, 65 (1967); L. M. Beyer, G. Berzins, and W. H. Kelly, *ibid.* **A93**, 436 (1967).
[35] A. H. Wapstra, G. J. Nijgh, and R. van Lieshout, in *Nuclear Spectroscopy Tables* (North-Holland Publishing Co., Amsterdam, 1959).
[36] C. F. Perdrisat, Rev. Mod. Phys. **38**, 41 (1966).
[37] J. R. Van Hise, G. Chilosi, and N. J. Stone, Phys. Rev. **161**, 1254 (1967).
[38] E. Yu. Berlovich, V. N. Klementyev, L. V. Krasnov, M. K. Kikitin, and I. Yurski, Nucl. Phys. **23**, 481 (1961).

TABLE VI. Weisskopf single-particle estimates for γ rays depopulating the high odd-parity states in Pr^{139}.

State energy (keV)	γ-ray energy (keV)	Relative intensity[a] (1%)	Single-particle estimate[b] for $t_{1/2}$ (sec) (corrected for conversion) $E1$	$M1$	$E2$
1624.5	101.3	6.5	1.1(−13)	1.6(−11)	3.8(−7)
	254.9	20	9.5(−15)	1.4(−12)	5.1(−9)
	601	6.5	7.8(−16)	1.1(−13)	7.6(−11)
	796.6	61	3.4(−16)	4.9(−14)	1.9(−11)
	802.4	≡100	3.3(−16)	4.8(−14)	1.8(−11)
1834.1	209.7	9.0	1.6(−14)	2.3(−12)	1.3(−8)
	810.1	23	3.2(−16)	4.7(−14)	1.7(−11)
	982.2	≡100	1.8(−16)	2.6(−14)	6.6(−12)
	1006.1	12	1.7(−16)	2.4(−14)	5.8(−12)
	1011.9	10	1.7(−16)	2.4(−14)	5.7(−12)
1927.1	92.9	89	8.2(−14)	1.2(−11)	3.3(−7)
	302.7	14	5.8(−15)	8.4(−13)	2.2(−9)
	403.9	86	2.5(−15)	3.7(−13)	5.4(−10)
	1075.1	≡100	1.4(−16)	2.0(−14)	4.2(−12)
	1105.2	77	1.3(−16)	1.8(−14)	3.6(−12)
2048.8	214.6	33	1.5(−14)	2.2(−12)	1.1(−8)
	424.3	39	2.2(−15)	3.2(−13)	4.3(−10)
	1024.6	72	1.6(−16)	2.3(−14)	5.3(−12)
	1220.9	≡100	9.5(−17)	1.4(−14)	2.2(−2)
	1226.9	83	9.3(−17)	1.3(−14)	2.2(−12)
2174.3	340.4	18	4.2(−15)	6.0(−13)	1.3(−9)
	1322.4	46	7.4(−17)	1.1(−14)	1.5(−12)
	2060.4	≡100	2.0(−17)	2.8(−15)	1.6(−13)
2196.7	147.9	57	3.7(−14)	5.4(−12)	5.9(−8)
	362.6	≡100	3.5(−15)	5.0(−13)	9.21(−10)
	572.1	26	9.1(−16)	1.3(−13)	9.7(−11)
	673.5	39	5.6(−16)	8.0(−14)	4.3(−11)
	1344.8	22	7.1(−17)	1.0(−14)	1.4(−12)
	1374.7	30	6.6(−17)	9.5(−15)	1.2(−12)

[a] The strongest γ ray from each level is arbitrarily given a relative intensity of 100% and the others are compared with this.

[b] Reference 29 as treated in Ref. 34.

branching ratio would also favor $\frac{9}{2}+$ ($M1$, $E2$ versus pure $E2$) over $\frac{7}{2}+$ (both $M1$, $E2$), but, as pointed out in connection with the 828.1-keV state, one has to know more about the internal structures of such states before other than gross decisions based on branching ratios can be made.

On the basis of the 910.2-keV γ to the $\frac{7}{2}+$ 113.8-keV state, a γ ray that is at least five times as intense as the unobserved 1024.0-keV ground-state γ ray, one can probably limit the spins of the 1024.0-keV state to a range of two units on either side of $\frac{7}{2}$. Because the state competes favorably for feeding from the 1624.5-, 1834.1-, and 2048.8-keV states, which again are fed directly by $\frac{11}{2}-$ Nd^{139m}, this range is biased toward the high-spin side of $\frac{7}{2}$. Finally, the lack of direct ϵ population (upper limit $\approx$0.4%) suggests even parity. Conclusion: $(\frac{5}{2}+)$, $\frac{7}{2}+$, $\frac{9}{2}+$, or $\frac{11}{2}+$ for this state.

E. High Odd-Parity States

The most intriguing aspect of this study is the population of (at least) six high-lying states in Pr^{139} by what appear to be allowed transitions from $\frac{11}{2}-$ Nd^{139m}. These six states, at 1624.5, 1834.1, 1927.1, 2048.8, 2174.3, and 2196.7 keV, are populated by ϵ decay with logft's that range from 5.6 to 6.3. This would seem to imply that these states have spins of $\frac{9}{2}$, $\frac{11}{2}$, or $\frac{13}{2}$, all with *odd* parity. Granted that logft values by themselves are not always reliable indicators of the degree of forbiddeness in β decay, still it is much more common for allowed transitions to be abnormally slow than for first-forbidden transitions to be abnormally rapid.[39] Also, the decay to the presumed $h_{11/2}$ 821.9-keV state should be, superficially at least, the most straightforward of the β-transitions from Nd^{139m}, and it has a logft of 7.0. Thus, these six high-lying states are favored for receiving population over the $h_{11/2}$ state. From this point of view, the ϵ decay to them is undoubtedly allowed. There are other indications, as well (to be described later), that they have odd parity. These six states also have other pecularities, among which are the large number of low-energy interconnecting γ transitions and the dearth of transitions to the low-lying states. In this section, we shall discuss these states somewhat phenomenologically, arriving only at estimates of the simplest external structures (i.e., spins and parities) consistent with our data, and will postpone the problems

[39] C. E. Gleit, C.-W. Tang, and C. D. Coryell, in *Nuclear Data Sheets*, compiled by K. Way *et al.* (U.S. Government Printing Office, National Academy of Sciences—National Research Council, Washington, D.C. 20418, 1963), NRC 5-5-109.

of detailed internal structure to Sec. IX, where it will be shown that they are three-quasiparticle states.

Now, although we have been perhaps overly conservative about drawing conclusions based on γ-ray branching ratios from the lower-lying states, the sheer number of competing γ rays from these high odd-parity states makes it a worthwhile endeavor to fathom at least whether or not useful information can be obtained by analyzing their various branchings. Consequently, we have assembled in Table VI the single-particle estimates for the $t_{1/2}$'s of all the γ rays originating from these states, assuming possible $E1$, $M1$, or $E2$ multipolarities. $M2$ and higher multipolarities were excluded on the basis of there being no likely mechanisms for enhancing them to the point that they could compete with the many possibilities for deexcitation by lower multipolarities. However, this tabulated information must be treated with circumspection, since the $E1$'s and $M1$'s could easily be retarded, as noted before; whereas, the $E2$'s could be either enhanced or not enhanced, depending on the collective or noncollective nature of the states involved Also, because we expect some common internal structure among these states, differences between $M1$ and $E2$ transition rates may not be predictable; therefore, our most useful information will be expected to come from comparing transitions that lead to states not in the group of six

Let us begin with the "prototype" state at 1834.1 keV. This state receives 37.4% of the ϵ decay, with $\log ft=5.6$, and the argument for its being $\frac{9}{2}-$, $\frac{11}{2}-$, or $\frac{13}{2}-$ is clearly stronger than for any of the other states. Of the five γ rays that deexite it, the intense 982.2-keV γ to the 851.9-keV state seems rather unambiguously to be an $E1$ (Table V, Fig. 9). This is additional evidence for odd parity, as we previously assigned the 851.9-keV state $\frac{9}{2}+$ or possibly $\frac{7}{2}+$. The $\frac{9}{2}+$ assignment would imply either $\frac{9}{2}-$ or $\frac{11}{2}-$ for the 1834.1-keV state, while the $\frac{7}{2}+$ assignment would limit it to $\frac{9}{2}-$.

At this point we can only check the consistency of the other γ rays with these assignments. The 1006.1-keV γ to the $(\frac{7}{2}+, \frac{9}{2}+)$ 828.1-keV state presumably is a parity-changing transition like the 982.2-keV γ, whereas the 1011.9-keV γ to the $\frac{11}{2}-$ 821.9-keV state is not. The simplest explanation is for the 1011.9-keV γ to be $M1$ and the 1006.1-keV γ to be $E1$. The pronounced difference in the rates of the 982.2- and 1006.1-keV "$E1$" γ's must be attributed to internal structures of the states. (We shall see later that there are strong implications that the transitions out of the high odd-parity multiplet are rather highly hindered, so small admixtures in the states involved could have strong effects on the transition rates.) Remembering that the latter is compatible with $\frac{7}{2}+$ for the 828.1-keV state, we are left with $\frac{9}{2}-$ and $\frac{11}{2}-$ for the 1834.1-keV state.

The relatively intense 810.1-keV γ would also appear to be an $E1$, allowing us to remove the $\frac{5}{2}+$ possibility for the 1024.0-keV state. The $M1$ and/or $E2$ assignment (Table V, Fig. 9) for the 209.7-keV γ adds nothing new, but we note that the 1624.5-keV state must be quite similar to the 1834.1-keV state for this transition to be so enhanced.

Arguments for the 1927.1-keV state, which receives 12.8% of the ϵ population, follow along similar lines. In particular, the 92.9-keV transition must be a collectively-enhanced $M1$ and/or $E2$, making the 1927.1- and 1834.1-keV states quite similar in origin. The 1105.2-keV γ to the 821.9-keV state may be $M1$, and the 1075.1-keV γ to the 851.9-keV state may be $E1$, all of which is consistent with $\frac{9}{2}-$ or $\frac{11}{2}-$ (equally probable) for the 1927.1-keV state. An educated guess for the 403.9-keV γ is $E1$, which would imply positive parity for the 1523.2-keV state.

The 2196.7-keV state also appears to be very closely related to the 1834.1-keV state, viz., the strong 362.6-keV γ. Arguments parallel those above, resulting in $\frac{9}{2}-$ or $\frac{11}{2}-$ as possible choices.

The 1624.5- and 2048.8-keV states are akin in that both favor depopulating to the 828.1- rather than the 851.9-keV state. In each case what would appear to be an $M1$ transition to the $\frac{11}{2}-$ 821.9-keV state competes most favorably with an apparent $E1$ to the 828.1-keV state. Arguments for odd parity are also weakest for these two states ($\log ft=6.3$ for ϵ decay to each), but the deexcitation pattern is no easier to interpret were we to assume high-spin even-parity states. Thus, we tentatively choose $\frac{9}{2}(-)$ or $\frac{11}{2}(-)$ as possible assignments. It is perhaps worth noting that, if our assignments are correct and the six "high odd-parity" states are indeed closely related, there seems to be an interesting gradation in properties, with the 1834.1-keV state standing toward the middle, being the only state directly connected to all the others by γ transitions. One example of this gradation is the strong transition between the 1927.1- and 1834.1-keV states, between the 1834.1- and 1624.5-keV states, and (less strong) between the 1624.5- and 1369.6-keV states—this contrasts with the weak transition between the 1927.1- and 1624.5-keV states and the absence of a transition (upper limit $\approx 0.2\%$) between the 1927.1- and 1369.6-keV states. (This sort of behavior ought to aid in sorting the states when shell-model calculations are done on our proposed three-quasiparticle configuration for these states.)

The 2174.3-keV state stands somewhat apart from the other five in that it is the only one to deexcite directly to the lowest states in Pr^{139} and to miss populating several of the other five with quite intense γ rays. Its large ϵ population ($\log ft=5.9$) does, however, indicate $\frac{9}{2}-$, $\frac{11}{2}-$, or $\frac{13}{2}-$. And its 2060.4-keV γ to the $\frac{7}{2}+$ 113.8-keV state, 1322.4-keV γ to the $(\frac{9}{2}+, \frac{7}{2}+)$ 851.9-keV state, and lack of a transition (1352.4-keV γ $\lesssim 0.3\%$) to the $\frac{11}{2}-$ 821.9-keV state favor the $\frac{9}{2}-$ assignment. The presence of the 2060.4-keV γ also implies, if it is a three-quasiparticle state, that this state includes some $\pi g_{7/2}$ character in its composition, thus being less "pure" than the other five.

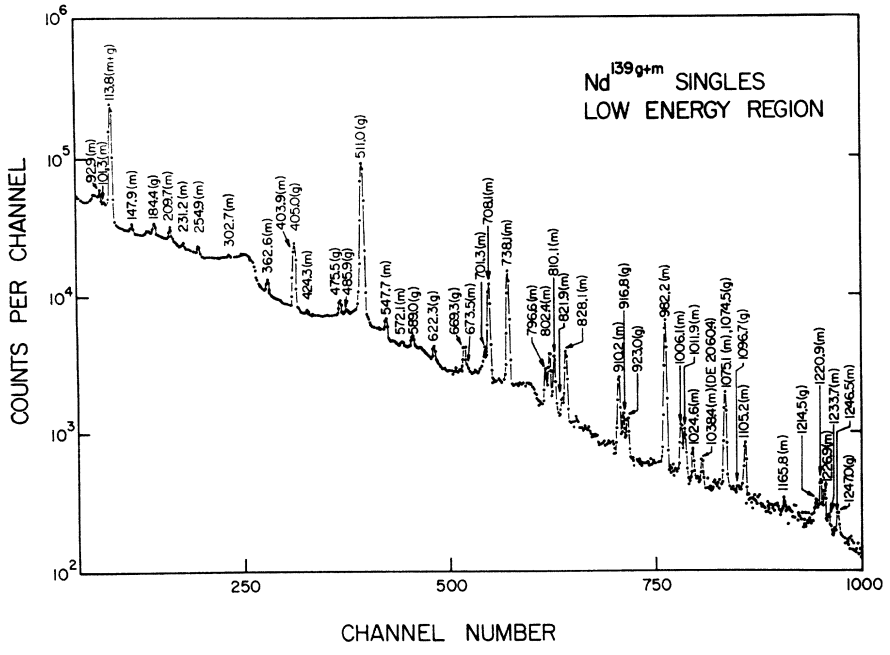

FIG. 11. (a) Nd^{139g+m} singles γ-ray spectrum taken with a 7-cm^3 Ge(Li) detector—low-energy portion. This spectrum is the sum of six $\approx$20-min runs taken $\approx$30 min after the end of 45-sec proton bombardments. In this way, the Nd^{139g} contribution was maximized both with respect to short-lived contaminants and with respect to Nd^{139m}. (b) Nd^{139g+m} singles γ-ray spectrum taken with a 7-cm^3 Ge(Li) detector—high-energy portion.

F. Remaining States

The only remaining states in Pr^{139} excited by Nd^{139m} ϵ decay that were known with enough assurance to be placed in the decay scheme are the 1369.6- and 1523.2-keV states. The 1369.6-keV state receives 1.3% of the ϵ decay, with $\log ft = 7.3$. Thus, one cannot decide between allowed and first-forbidden nonunique decay, and the assignment can be $\frac{9}{2}\pm$, $\frac{11}{2}\pm$, or $\frac{13}{2}\pm$. Even less can be said about the 1523.2-keV state which receives no direct population from Nd^{139m}. On the basis of the strength of the 101.3-keV γ from the 1624.5-keV state, a weak argument can be made for spins between $\frac{7}{2}$ and $\frac{13}{2}$ with perhaps even parity.

VI. EXPERIMENTAL RESULTS FOR Nd^{139g}

A. γ-Ray Singles Spectra

A γ-ray singles spectrum of Nd^{139g+m} taken with the 7-cm^3 Ge(Li) detector described in Sec. III A is shown in Figs. 11(a) and 11(b). This spectrum represents the sum of six runs taken $\approx$30 min after the end of $\approx$45-sec proton bombardments. The duration of each of these

runs was $\approx$20 min. Spectra were recorded periodically as the sources aged in order to identify activities with different half-lives and to follow the Ng^{139g} as it reached equilibrium with Nd^{139m}. Most of the γ-ray intensity, even this soon after the bombardments, originates from Nd^{139m} decay, for some 88% of Nd^{139g} β decay proceeds directly to the ground state of Pr^{139}.

A list of the energies and relative intensities of the γ rays identified with the decay of Nd^{139g} is given in Table VII. These were measured as described in Sec. III A except that the now well-determined Nd^{139m} γ ray energies were used as internal calibration standards. Of the 21 γ rays listed in Table VII, only the 405.0-keV γ has been reported previously.[7]

A basic cause of experimental difficulties encountered in the study of Nd^{139g} decay is that the annihilation photons are an order of magnitude more intense than any of the γ rays following its decay. This means that even the low activity of 5.5-h Nd^{139m} produced by our 45-sec bombardments significantly masks the 30-min Nd^{139g} γ rays shown in Figs. 11(a) and 11(b).

As mentioned briefly in Sec. II, an attempt was made to populate Nd^{139g} selectively apart from Nd^{139m} by using the

$$Pr^{141}(\tau, 5n)Pm^{139} \xrightarrow{\beta^+/\epsilon} Nd^{139g}$$

reaction. We expected that the ground state of Pm^{139} would be a $\frac{5}{2}+$ state and would populate $\frac{3}{2}+$ Nd^{139g} in preference to $\frac{11}{2}-$ Nd^{139m}, thus producing a cleaner spectrum. The attempt was a partial success because the Nd^{139g}/Nd^{139m} isomer ratio was indeed increased by an order of magnitude. However, the presence of many other short- and long-lived contaminants from competing reactions nullified any net advantage of this method for producing clean Nd^{139g} sources. One would need to use this reaction in conjunction with a rapid ion-exchange separation (not yet feasible but perhaps available within a few years) for it to be really clean. It did, however, verify the relative intensities of most of the Nd^{139g} γ rays. (The resulting spectra are displayed in Ref. 19.)

B. γ-γ Coincidence Studies

By analogy with the decay scheme[9] of $d_{3/2}$ Nd^{141}, we expected that a number of states would be present, which, upon receiving direct β population, would deexcite directly to the Pr^{139} ground state. For this reason we used the 8×8-in. NaI(Tl) split annulus[18] and a 3×3-in. NaI(Tl) detector in an anticoincidence experiment with the 7-cm^3 Ge(Li) detector; the geometry was as described in Sec. III B. Again, the single-channel analyzer for the NaI(Tl) detectors was set so that the gate would be active for all γ rays above 100 keV. The resulting anticoincidence spectrum is shown in Fig. 12, and the resulting intensities of the Nd^{139g} γ rays (relative to 100 for the 738.1-keV Nd^{139m} γ ray) are listed in Table VIII. Seven states in Pr^{139} were indicated by these results.

TABLE VII. Energies and relative intensities of γ rays observed in Nd^{139g} spectra.

Measured γ-ray energy (keV)	Relative γ-ray intensity[a]
113.8±0.2	10.1±10[b]
184.4±0.4	4.2±0.4
405.0±0.4	36.4±3.0[c]
475.5±0.4	7.9±0.6
485.9±0.8	2.8±0.7
511.0($\gamma^{\pm}$)	360±50[d]
589.0±0.5	5.3±0.6[e]
622.3±0.3	6.4±1.0
669.3±0.5	8.3±2
916.8±0.4	8.5±0.6
923.0±0.4	6.9±0.8
1074.5±0.5	11.9±1
1096.7±1.0	0.9±0.4
1214.5±0.4	2.2±0.3
1247.0±1.0	0.6±0.3
1311.8±0.6	2.0±0.7
1328.4±0.6	1.1±0.3
1405.5±0.7	3.3±0.5
1449.5±0.7	0.8±0.3
1464.1±0.5	2.3±0.4
1500.8±0.8	2.0±0.5
1531.2±1.0	1.1±0.4

[a] Relative to 100 for the intensity of the 738.1-keV γ ray in Nd^{139m} $\approx$30 min after the end of $\approx$45-sec proton bombardments.

[b] Based on sum of γ intensity feeding 113.8-keV level as indicated in decay scheme (Fig. 8) because most of the 113.8-keV γ intensity originates from population by the 5.5-h Nd^{139m}, even 30 min after Nd^{139m+g} is produced.

[c] Result after the 403.9-keV component of the 403.9-, 405.0-keV doublet is subtracted out on the basis of the Nd^{139m} relative intensities (see Table I).

[d] Approximately 98% of the annihilation photons come from Nd^{139g} decay $\approx$30 min after the production of Nd^{139m+g}.

[e] From the decay scheme we can only place an upper limit of 16.1 on the intensity of a hypothetical 511.8-keV γ ray depopulating the 916.8-keV state.

In order to complement the anticoincidence data, a coincidence spectrum was obtained using the same apparatus. The gate from the NaI(Tl) detectors was open for γ rays above 350 keV. This "integral" coincidence spectrum is shown in Fig. 13(a), and the relative intensities derived from it are also included in Table VIII. As expected, they verify the results of the anticoincidence data.

The high intensity of the 405.0-keV γ suggests the presence of a state in Pr^{139} at this energy. Four energy sums also indicate possible γ-ray cascades involving this transition. To obtain evidence supporting these cascades, we gated the NaI(Tl) annulus detector on the 380–430-keV region and displayed the coincident spectrum seen by the 7-cm^3 Ge(Li) detector. The resolving time (2τ) of the coincidence circuit was $\approx$100 nsec. This spectrum is shown in Fig. 13(b), and the relative intensities of the Nd^{139g} γ rays are included in Table VIII, where the ones that are thought to be in coincidence with the 405.0-keV γ are so indicated.

The same coincidence spectrometer was then gated on the 113.8-keV γ. The measured relative intensities from the resulting spectrum[19] are also listed in Table VIII. This experiment verified the energy-sum indication that the 113.8-keV γ is in cascade with the 475.5- and 1214.5-keV γ's.

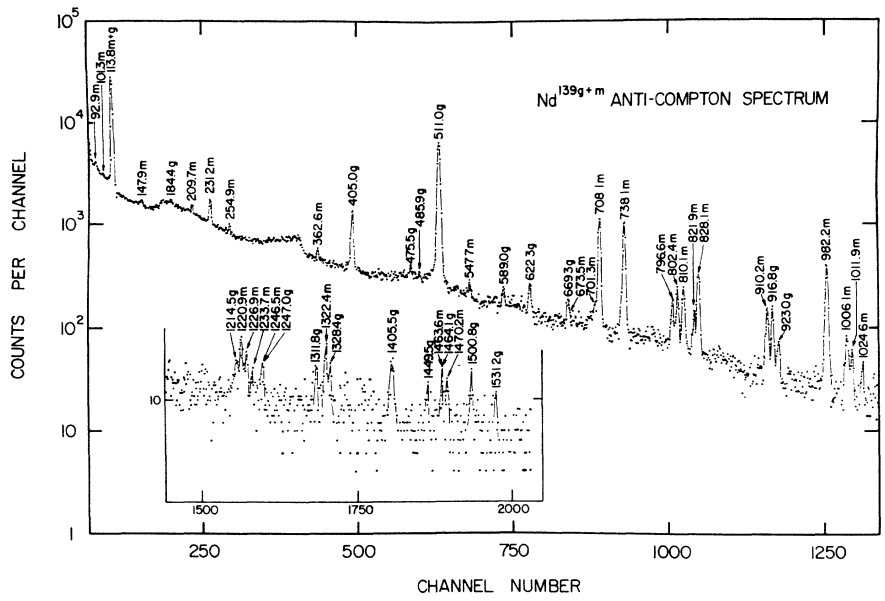

FIG. 12. Nd^{139g+m} anticoincidence spectrum. (cf. Fig. 2.)

Confirmations of several of the coincidences described above and new evidence for a 405.0–184.4-keV cascade were obtained with a 3×3-in. NaI(Tl) 7-cm³ Ge(Li) two-parameter (megachannel) spectrometer employing dual 4096-channel ADC's. These data are summarized in Table VIII. Following each coincident event, the channel numbers representing the photon energies were stored in a dedicated buffer in our SDS Sigma 7 computer. When the buffer filled, its contents were written on magnetic tape. We were then able to recover the coincidence information in slices in order to construct useful spectra. In Fig. 14(a), we show the integral Nd^{139g+m} coincidence spectrum obtained on the Ge(Li) side, and in Fig. 14(b) we show the results of gating on the 405-keV region of the NaI(Tl) side and displaying the resulting Ge(Li) spectrum.

TABLE VIII. Relative intensities of photons in the decay of Nd^{139g} observed in several γ-γ coincidence experiments.

		Relative intensity					
E_γ	Fig. 11 singles[a]	Fig. 12 anti-coincidence	Fig. 13 integral coincidence	Fig. 14 405-keV coincidence	Ref. 16 113.8-keV coincidence	Fig. 15a 2-d integral coincidence	Fig. 15b 2-d 405-keV coincidence
113.8	10.1	<24	...	...	...	<160	<231
184.4	4.2	<0.3	5.8[d]	...	...	4.8[d]	27[d]
405.0	36.4	<9.8	<49[d]	18	<17	35[d]	44
475.5	7.9	0.7	8.1[d]	5.2	11[d]	6.3[d]	...
485.9	2.8	0.5	2.7[d]	4.0[d]	<3	1.8[d]	24[d]
511.0[b]	360	120	304	127	360	78	287
(511.8?	<16.1?)	...	...	...	...	...	...
589.0	5.3	1.6	4.8	<9.8	<5	...	...
622.3	6.4	2.8	0.8	<8	<5	<2	...
669.3	8.3	1.8	1.4[d]	18[d]	<6	8[d]	61[d]
916.8	8.5	5.1[c]	0.3	1.9	<4	<1	...
923.0	6.9	1.0	0.8[d]	17[d]	<5	3[d]	41[d]
1074.5	11.9	8[c]	<1	<11	<13	<15	...
1096.7	0.9	<0.9	0.7[d]	2[d]	...	...	...
1214.5	2.2	0.5	<1	2	5	...	...
1247.0	0.6	<0.6	<0.6	<6.5	...	...	...
1311.8	2.0	0.8[c]	<0.3	<3	...	...	...
1328.4	1.1	0.5[c]	<0.3	<10	...	...	...
1405.5	3.3	2.3[c]	0.1	<3	...	...	...
1449.5	0.8	0.55[c]	0.1	<3	...	...	...
1464.1	2.3	<1.0	<0.6	<3	...	...	...
1500.8	2.0	1.2[c]	<0.2	<3	...	...	...
1531.2	1.1	0.4	<0.2	<3	...	...	...

[a] Intensities relative to 100 for the intensity of the 738.1-keV γ in Nd^{139m} ≈30 min after the end of 45-sec proton bombardments.

[b] Largely composed of annihilation photons, but an admixture of 511.8-keV γ's with an intensity of ≤16, using the scale of Table V, has not been ruled out. This possibility is discussed in Sec VII.

[c] Evidence seen here for primarily ϵ-fed ground-state transition.

[d] Evidence seen here for γ-γ coincidence event.

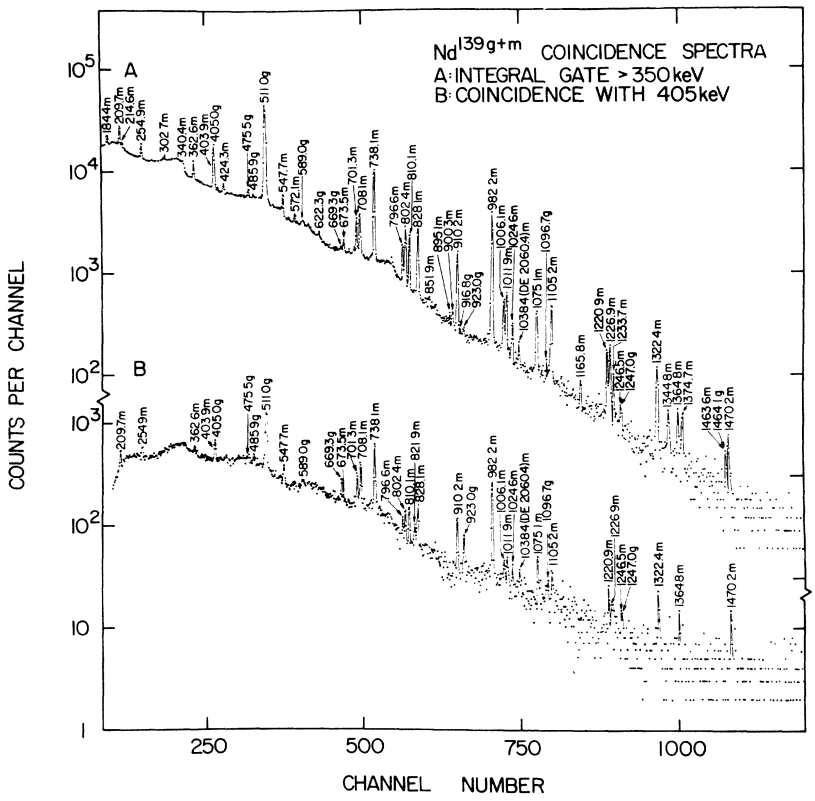

FIG. 13. (a) Nd^{139g+m} integral coincidence spectrum. This spectrum was recorded by a 7-cm³ Ge(Li) detector with the 8×8-in. NaI(Tl) split annulus set to accept all γ rays above 350 keV. (b) The annulus gate was set on the 405-keV energy region.

VII. Nd^{139g} DECAY SCHEME

The decay scheme for Nd^{139g} that we were able to deduce from our measurements was presented in Fig. 8 for comparison with the Nd^{139m} decay scheme. Again, all transition energies and excited state energies are given in keV and the β^+/ϵ ratios are calculated values.[21] All of the (total) transition intensities are given in percent of the Nd^{139g} disintegrations.

None of the ten excited states we propose has been reported previously in published Nd^{139g} decay-scheme studies. The only one of these states for which we also have evidence of population from Nd^{139m} decay (i.e., β decay) is the 113.8-keV state. The 113.8-keV γ was seen to have a 30-min decay component in addition to its dominant 5.5-h component. It was also observed to be in cascade with the 475.5- and 1214.5-keV γ's accompanying Nd^{139g} decay.

We mentioned earlier that the high intensity of the 405.0-keV γ indicates the probability of a state in Pr^{139} at 405.0 keV. This placement was confirmed by coincidences of four γ rays (five, if we include a tentative 511.8-keV γ) with the 405.0-keV γ. In the process of constructing the decay scheme, we assumed that the imbalance of γ-ray intensities leaving and entering the 405.0-keV state is removed entirely by β feeding of this state. However, we cannot rule the possibility that a 511.8-keV transition from a level at 916.8 keV to this state is present ($\leq 2.5\%$) but obscured by the intense annihilation photons.

Higher-lying states at 589.2, 1074.4, 1328.2, and 1501.2 keV are suggested by energy sums and relative photon intensities and confirmed by coincidence and anticoincidence information. The states at 916.8, 1311.8, 1405.5, and 1449.5 keV were placed on the basis of the enhancement (reduction) of the 916.8-, 1311.8-, 1405.5-, and 1449.5-keV γ's in anticoincidence (coincidence) experiments as seen in Figs. 12–14 and Table VIII.

The $Q_\epsilon = 2800$ keV is a calculated value,[20] which ought to be good to within several hundred keV. There have been several attempts to measure the β^+ end points, but at this time their precision is not particularly good. Several measurements of the (total) annihilation photon relative intensity component due to Nd^{139g} were used in order to calculate the 88% β branching to the ground state. In the $Nd^{139m+g} \rightarrow Pr^{139} \rightarrow Ce^{139}$ decay chain, Nd^{139g} accounts for $\approx 98\%$ of the annihilation photon intensity at ≈ 30 min after the 45-sec bombardments.

Four unplaced γ rays identified with Nd^{139g} decay were observed with energies (relative intensities) of 622.3 (6.4), 1247.0 (0.6), 1464.1 (2.3), and 1531.2 keV (1.1). The sum of these intensities yields 8.3% of the observed Nd^{139g} γ-ray intensity and 1.5% of the observed Nd^{139g} total disintegrations. Some properties of these γ rays can be deduced from Tables VII and VIII. The relatively strong 622.3-keV γ perhaps suggests placing a state at 622.3 keV; but, in view of the lack of any supporting evidence, we have omitted this from the decay scheme. The logft for population of such a state would be $\gtrsim 6.8$.

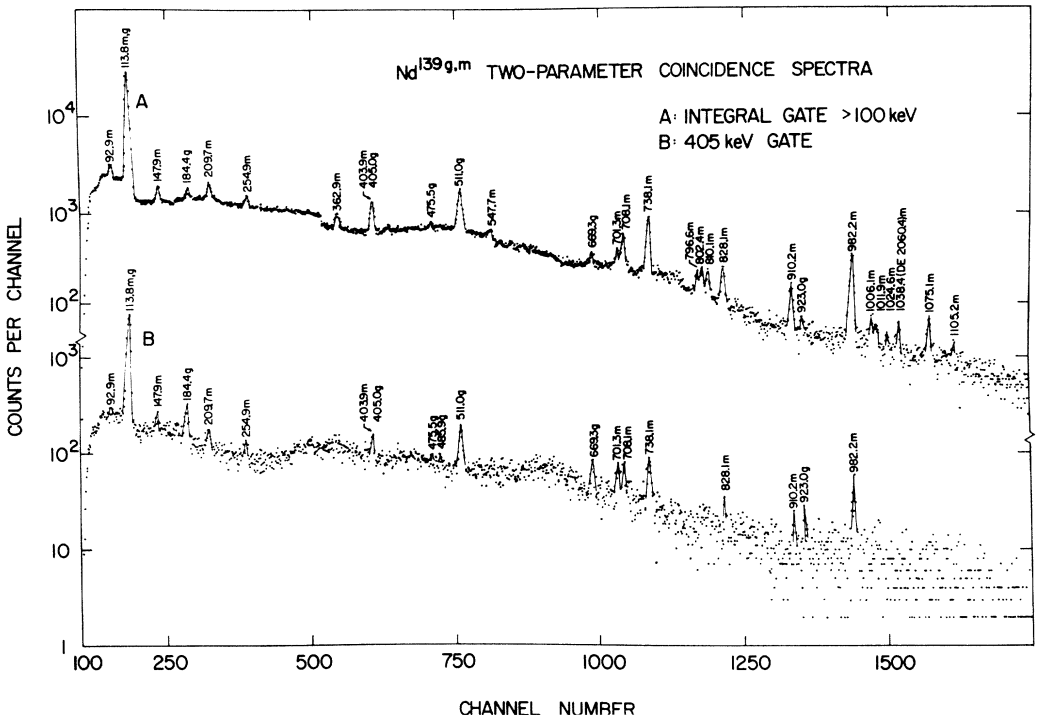

FIG. 14. Slices from two-dimensional (megachannel) γ-ray spectrum for Nd^{139g+m}. (A) Integral gate of all γ rays above 100 keV. (B) 405-keV gate. See the text for details.

VIII. SPIN AND PARITY ASSIGNMENTS FROM Nd^{139g} DECAY

Spin and parity assignments to the lowest two levels have been discussed in Sec. VI C in connection with the decay of Nd^{139m}. The 63% ϵ, 27% β^+ decay to the ground state is quite consistent with a $\pi d_{5/2} \rightarrow \nu d_{3/2}$ transition, and the $\log ft = 5.1$ is remarkably close to that found for the analogous transition in Nd^{141} decay[9] ($\log ft = 5.3$).

It is difficult to set a precise upper limit on direct β decay to the $\frac{7}{2}+$ 113.8-keV state because of the intense 113.8-keV γ-ray component from Nd^{139m} decay. Following the analogy with the much cleaner Nd^{141} decay, there we could place an upper limit of 0.03%, with $\log ft > 8.8$. For Nd^{139g} decay, of course, such precision is out of the question, but the fact that we see no indication of direct β population is clearly consistent with a $(d_{5/2})^2(g_{7/2})^{-1}$ configuration, as discussed before.

The remaining nine levels all are populated by β^+/ϵ decay from $\frac{3}{2}+$ Nd^{139g} with $\log ft$'s ranging from 5.6 to 7.2. These all fit quite nicely in the range expected for allowed decay, and, although one cannot rule out first-forbidden decay on the basis of these alone, we see no indication that we need postulate anything other than $\frac{1}{2}+$, $\frac{3}{2}+$, or $\frac{5}{2}+$ states as being populated directly by Nd^{139g}. Indeed, all the $\log ft$ values are actually slightly smaller than for the analogous transitions in Nd^{141} decay.[9] For some of the states, especially those exhibiting γ-ray branching, we can perhaps narrow the assignments further.

The states at 405.0 and 916.8 keV are tentatively assigned $\frac{1}{2}+$ or $\frac{3}{2}+$ because they both decay to the $\frac{5}{2}+$ ground state and miss the $\frac{7}{2}+$ 113.8-keV state. The 916.8-keV state may or may not decay also to the 405.0-keV state via the unobserved 511.8-keV transition, which just might have appreciable intensity. This fact is more concerned with the internal structure of (both) states than with their spin and parity—although the presence of the transition would lend further support to our assignments. Solely on the prediction of the shell model that the $s_{1/2}$ state ought to lie between the $h_{11/2}$ state and the $d_{5/2}$ and $g_{7/2}$ states, one is tempted to identify the 405.0-keV state with it. There is no supporting evidence, however, and one must ask why the $s_{1/2}$ state should be populated so easily here when it has not been seen in either Nd^{141} decay[9] or Ce^{143} decay[40] to the next heavier Pr isotopes, which otherwise show much the same single-particle state positions (within a few hundred keV). We shall also see that γ-ray branchings to this state tend to support the $\frac{3}{2}+$ rather than the $\frac{1}{2}+$ assignment.

Next we consider the states that decay through the $\frac{7}{2}+$ 113.8-keV state, namely, those at 589.2 and 1328.2 keV. The mere presence of the 475.5- and 1328.4-keV γ's rules out the $\frac{1}{2}+$ possibility for these states. We can tentatively narrow both assignments down to $\frac{5}{2}+$ with the aid of the γ-ray branchings.

For the 589.2-keV state, a $\frac{3}{2}+$ assignment would lead to single-particle estimates[35] of the relative intensities of the 589.0:475.5:184.4-keV γ's ($M1:E2:M1$, with possible $E2$ admixing in the $M1$'s) of 1:0.005:0.04. A $\frac{5}{2}+$ assignment (all $M1$'s) would lead to roughly 1:0.5:0.06. Although considerable $E2$ enhancement is

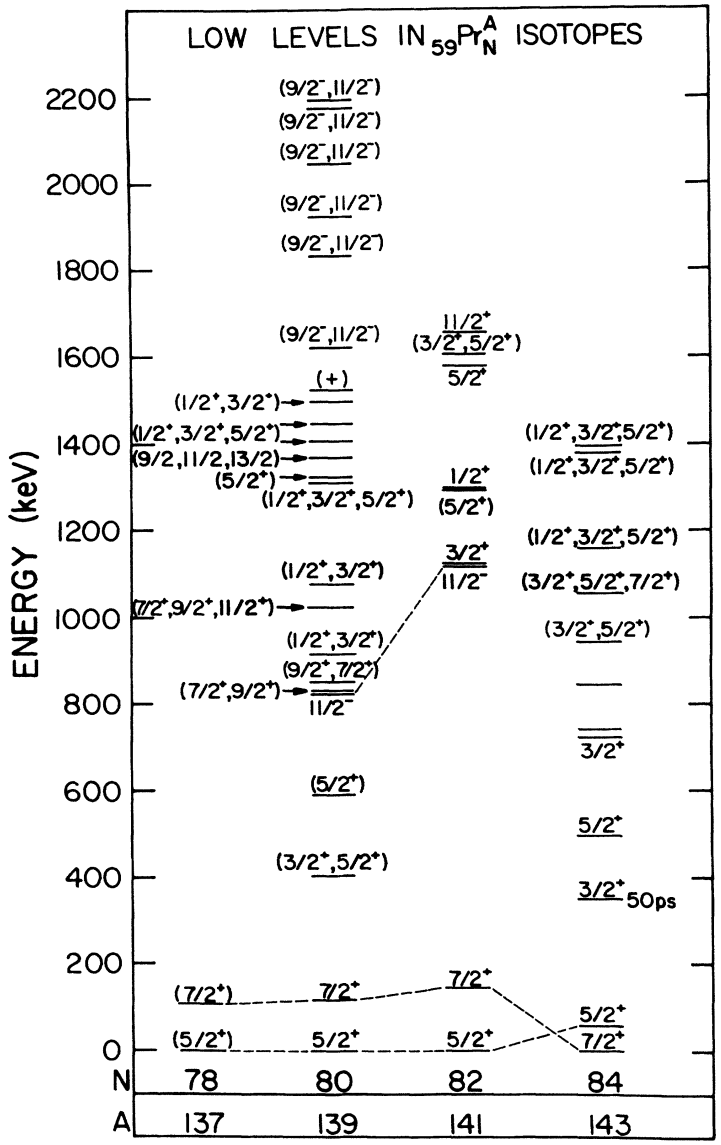

FIG. 15. Experimental levels in odd-mass Pr isotopes demonstrating the effects of changing neutron number on the positions of the states. Unambiguously related states are connected by the dashed lines. References: Pr^{137}, Ref. 22; Pr^{139}, this study; Pr^{141}, Refs. 9, 41, and 42; and Pr^{143}, Ref. 40.

to be expected (because of the softness of this nucleus to vibrations) and $M1$'s might be somewhat retarded, the latter ratio is clearly preferable when compared with the experimental ratio, 1:1.5:0.75. The 405.0- and 589.2-keV states may well be core-coupled states involving the $d_{5/2}$ ground state. That they lie so low is not too surprising, for Pr^{139} (two neutrons fewer than 82) should be somewhat analogous to Pr^{143} (two neutrons more than 82),[40] which, being again somewhat soft to vibrational excitations, appears to have core-coupled states at this same energy. A $\frac{5}{2}+$ assignment for the 589.2-keV state would exclude a $\frac{1}{2}+$ assignment for the 405.0-keV state.

Quite similar reasoning holds for the 1328.2-keV state, except that it lies high enough that one can deduce little about its internal makeup. The corresponding single-particle predictions for the relative intensities of the 1328.4:1214.5:923.0-keV γ's are 1:0.005:0.3 and 1:0.8:0.3 for $\frac{3}{2}+$ and $\frac{5}{2}+$ assignments, respectively. Although neither can be called a satisfactory fit (experimental ratios are 1:1.5:5.5), the latter is in the ball park. Considering the obvious enhancement of the γ rays to the 405.0-keV state from both the 1328.2- and 589.2-keV states, one is tempted to look for the 739.0-keV γ between the latter two. Unfortunately, the presence of the intense 738.1-keV γ from Nd^{139m} decay precludes our seeing it, and it could be as intense as 0.7% and have excaped detection.

The states at 1074.4 and 1501.2 keV are tentatively assigned $\frac{3}{2}+$ because they hit the ground state but miss the $\frac{7}{2}+$ 113.8-keV state in their depopulation. This is indeed tentative, however, and one must know more about the internal structure of these states before firm

[40] P. R. Gregory, L. Schellenberg, Z. Sujkowski, and M. W. Johns, Can. J. Phys. **46**, 2797 (1968); K. P. Gopinathan, Phys. Rev. **139**, B1467 (1965).

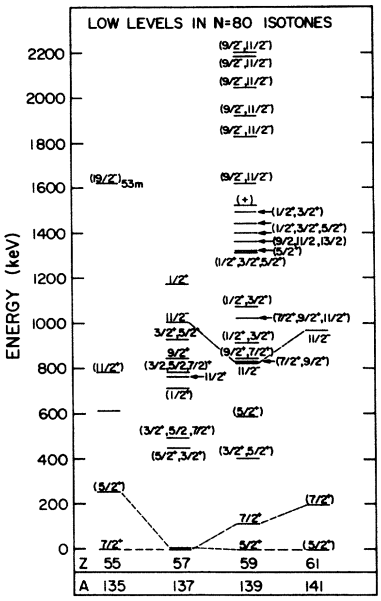

FIG. 16. Experimental levels in odd-mass $N=80$ isotones, demonstrating the effects of changing proton number on the positions of the states. Unambiguously related states are connected by the dashed lines. References: Cs^{135}, Ref. 43 and S. Thulin, Arkiv Fysik **9**, 137 (1955); La^{137}, Ref. 28; Pr^{139}, this study; and Pm^{141}, Ref. 7 and R. Eppley, R. Todd, D. B. Beery, W. H. Kelly, and Wm. C. McHarris (unpublished).

assignments can be made. It would be quite possible, for example, to concoct a hypothetical $\frac{5}{2}+$ state consisting of a $d_{5/2}$ quasiparticle coupled to a 2+ phonon excitation that would clearly populate the ground state to the exclusion of the 113.8-keV state, straightforward multipolarity selection rules notwithstanding.

The remaining states, at 1311.8, 1405.5, and 1449.5 keV, which were placed on the basis of their ground-state transitions alone, might have their assignments narrowed down to $\frac{3}{2}+$ or $\frac{5}{2}+$; however, the population is quite weak for all three, with even parity even being somewhat in doubt, so we leave then as $\frac{1}{2}$, $\frac{3}{2}$, $\frac{5}{2}$ (+).

IX. DISCUSSION

A total of at least 23 states in Pr^{139}, practically none of which had been reported before, were observed from the combined decays of Nd^{139m} and Nd^{139g}. These states apparently can be classified in three quite distinct categories: (1) single-quasiparticle states, (2) single-quasiparticle states coupled to various vibrational configurations, and (3) three-quasiparticle states. Our conclusions can be most concrete about the states in the first category and, because of a rather unique feature in the β-decay properties of Nd^{139m}, the third category. As this is an experimental paper, our discussions that follow will remain empirical, but we indicate the directions, both experimental and theoretical, that might be taken for further elucidation of the properties of this most interesting nucleus.

A. Single-Particle States

Again, by "single-particle" states we mean merely those states with primarily single-quasiparticle amplitudes in their wave functions. These range from the more or less pure states near the ground to highly fractionated and complicated states at higher energies. When we speak of them in simple shell-model terms, this is not to imply that they are indeed pure shell-model states.

On the neutron-deficient side of $N=82$ in the lanthanide region, practically nothing has been done in the way of even qualitative calculations of the positions of nuclear states—even the pairing-plus-quadrupole force calculations of Kisslinger and Sorensen[32] give out at Nd^{141}. This means that we are forced to use empirical data for the mot part, although the sheer number of states excited in Pr^{139} in this study makes this more practicable than usual. Thus, in Figs. 15 and 16, respectively, we plot the known states in the light odd-mass Pr isotopes and in the odd-mass $N=79$ isotones. Here, we are beginning to get far enough from β stability that no scattering reactions have been done to excite states, so the number of states recorded is very much a function of Q_ϵ.

In Pr^{139} we probably see evidences of all the available single-proton states between $Z=50$ and $Z=82$. The most clearcut single-quasiparticle states are those at 0, 113.8, and 821.9 keV. The ground state undoubtedly consists primarily of a single $d_{5/2}$ proton outside a closed $g_{7/2}$ subshell, and the 113.8-keV state simply promotes a $g_{7/2}$ proton, resulting in $(d_{5/2})^2\ (g_{7/2})^{-1}$. As mentioned previously, the retarded $M1$ transition between them is characteristic of the l-forbidden $M1$'s between $g_{7/2}$ and $d_{5/2}$ states in a wide variety of nuclei in this region. The relatively small spacing between the first two states is consistent with trends in both proton and neutron numbers in neighboring nuclei, for the $\frac{7}{2}+$ and $\frac{5}{2}+$ states cross over between Pr^{141} and Pr^{143} and also between La^{137} and Pr^{139}.

The 821.9-keV state shows evidence of being a single $h_{11/2}$ proton outside the closed $g_{7/2}$ subshell. As mentioned in Sec. V D, the $M2$ transition from this state to the 113.8-keV state is retarded, while the $E3$ to the ground state is enhanced over single-particle estimates. Van Hise, Chilosi, and Stone[37] suggest that a similarly enhanced $E3$ transition in La^{137} could be explained in terms of a coupling of the $d_{5/2}$ proton to a 3− octupole vibration, resulting in a nearby $\frac{11}{2}-$ state that could be mixed into this state. Superficially, one might ask why it is not also possible to admix a similar $\frac{11}{2}-$ state, this time based on the $g_{7/2}$ proton, into this state, thereby enhancing the $M2$ as well as the $E3$ transition. As it turns out, one cannot really test either hypothesis, for the positions of possible octupole states are unknown. With our above shell-model assignments, however, the $E3$ is the better single-particle transition, involving principally the deexcitation only of a proton from the $h_{11/2}$ to the $d_{5/2}$ orbit. The $M2$, conversely, involves breaking the $g_{7/2}$ subshell in addition, so its retardation follows even on these simple arguments.

The positions of the $d_{3/2}$ and $s_{1/2}$ states are not so clear, but they are probably fragmented and contribute to

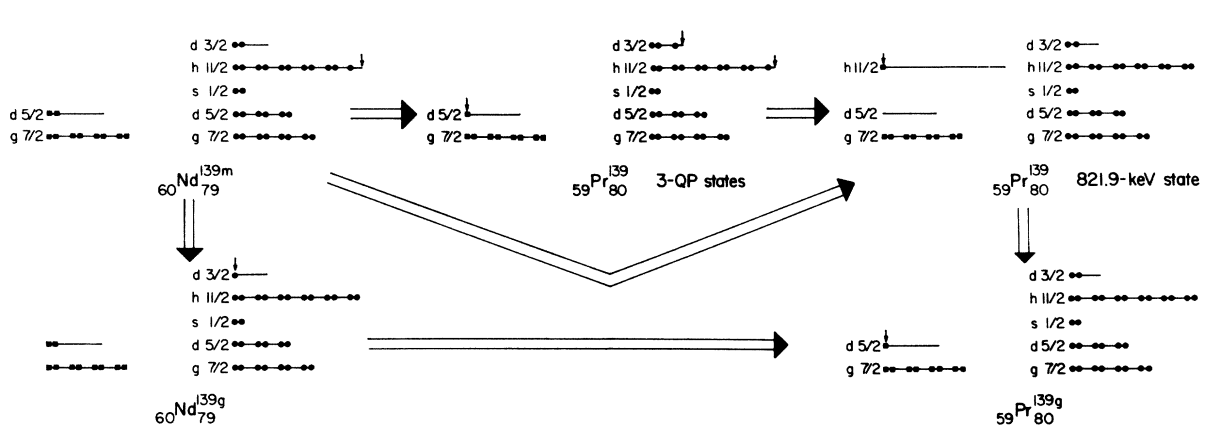

FIG. 17. Symbolic shell-model representations of some important transitions between Nd^{139} and Pr^{139} states. We have given a stylized picture of the proton (squares) and neutron (circles) states between 50 and 82 nucleons. The arrows point to the nucleons or holes of prime interest in each state.

several states above 1 MeV. The state at 405.0 keV (and at 589.2 keV, for that matter, if our spin assignments were incorrect) is not likely to be either of these single-particle states. In the more rigid Pr^{141}, other than the $g_{7/2}$ and $d_{5/2}$ states, there are no single-particle states below 1114 keV that were populated either by Nd^{141} decay[9] or by (τ, d)[41] or (d, τ)[42] scattering. Of the number of levels just above 1 MeV that were possible contenders, we were unable to identify specific levels with either the $d_{3/2}$ or $s_{1/2}$ states because of uncertainties connected with the vibrational character of that nucleus. Pr^{139} is much softer to deformations than Pr^{141}, and we thus expect many more low-lying states, but there is no reason to expect either the $d_{3/2}$ or $s_{1/2}$ states to drop drastically in energy, so they may be partly associated with a number of the higher levels.

B. Three-Quasiparticle States

In Sec. V E, we presented arguments to the effect that the six states at 1624.5, 1834.1, 1927.1, 2048.8, 2174.3, and 2196.7 keV appear to be high-spin odd-parity ($\frac{9}{2}-$ or $\frac{11}{2}-$) states. The only strightforward explanation we have found that will explain their enhanced ϵ population relative to the 821.9-keV state plus the many low-energy γ transitions among them and the dearth of direct transitions down to the ground or 113.8-keV states is that these six states are part of a three-quasiparticle multiplet having the configuration $(\pi d_{5/2})(\nu d_{3/2})^{-1}(\nu h_{11/2})^{-1}$. The particle transitions that we postulate are outlined in stylized form in Fig. 17.

In the extreme single-particle approximation, $_{60}Nd_{79}^{139g}$ can be represented as three $d_{3/2}$ neutron holes in the $N=82$ shell (i.e., a single neutron in the $d_{3/2}$ orbit) and eight $g_{7/2}$ (closed subshell) and two $d_{5/2}$ protons above $Z=50$. Owing to the isomeric properties discussed in Sec. V B, Nd^{139m} ought to differ only in the promotion of an $h_{11/2}$ neutron into the $d_{3/2}$ level, resulting in eleven $h_{11/2}$ and two $d_{3/2}$ neutrons. Now, there is nothing untoward about the decay of Nd^{139g} to the ground state of Pr^{139}, for the only change is the conversion of a $d_{5/2}$ proton into a $d_{3/2}$ neutron. This accounts for the low logft value of 5.1 for this transition.

The analogous transition from Nd^{139m}, i.e., $\pi d_{5/2} \rightarrow \nu d_{3/2}$, however, results in the three-particle configuration $(\pi d_{5/2})(\nu d_{3/2})^{-1}(\nu h_{11/2})^{-1}$. Hence, the apparent abnormally large population to these states is, in fact, the expected mode of decay. The 821.9-keV $\frac{11}{2}-$ state, on the other hand, should have the configuration $(\pi h_{11/2})(\nu d_{3/2})^2$, so decay to it would require converting one $d_{5/2}$ proton into an $h_{11/2}$ neutron, either in one step or perhaps through an intermediate $d_{3/2}$ neutron state, and a simultaneous promotion of the remaining $d_{5/2}$ proton to the $h_{11/2}$ state. The resulting relatively large logft of 7.0 is thus not unexpected.

Relatively few three-quasiparticle states are known, and these few are customarily produced by brute-force techniques (i.e., bombardments). Their recognition has hinged on an isomeric state now and then having a long half-life because of its high spin; for example, the nearby $\frac{19}{2}-$ isomer[43] at 1621 keV in Cs^{135} that could have either the same or a similar configuration as the states in Pr^{139}. It is worth noting that here we have somewhat unique mechanism for populating three-quasiparticle *multiplets* in a number of nuclei. The requirements are a high-spin nucleus, such as the $h_{11/2}$ isomers, and that it have sufficient decay energy to populate states above the pairing energy gap in its daughter nucleus. Additionally, the parent nucleus must be hung up with respect to decay by other modes; for example, an isomeric transition, if present, must be of sufficiently low energy to allow the ϵ decay to com-

[41] B. H. Wildenthal, R. L. Auble, E. Newman, and J. A. Nolen, Bull. Am. Phys. Soc. **13**, 1430 (1968).

[42] H. W. Baer and J. Bardwick, Bull. Am. Phys. Soc. **13**, 1430 (1968).

[43] L. B. Häller and B. Jung, Nucl. Phys. **52**, 524 (1964).

pete. Finally, the nucleus must have a relatively unique intrinsic configuration that forces the preferred decay path to be into the three-quasiparticle states. Such arrangements would appear to be present only for β^+/ϵ decay—further, they are likely to occur only below $N=82$. (Below $N=50$ the correct configuration occurs at Kr^{83} and Sr^{85}, but these are too close to β stability for populating high-lying states. Below $N=126$ the configuration is projected to occur around Pu^{211}, a region that is not even particle stable.)

Below $N=82$ the appropriate configurations can be found only at $N=79$ and $N=77$. On the neutron-rich side of $N=79$ there are, to be sure, some peculiar and complex decays of $\frac{11}{2}-$ isomers—e.g., Te^{131m} decays primarily to high-spin states at 1899 and 1980 keV[44]—but these cannot be pinned down as decay to three-particle states. On the neutron-deficient side, Ce^{137m} has a possible configuration, although it lacks the $d_{5/2}$ protons, so decay would be l forbidden ($\pi g_{7/2}\rightarrow\nu d_{3/2}$); however, its Q_ϵ is small enough to preclude such decay anyway.[45] This leaves Nd^{139m} as the nucleus closest to β-stability with the requisite properties. Other possible candidates in this region among currently known nuclei are $Sm^{141(m)}$ and $Nd^{137(m?)}$. These are now being investigated.

Although the above interpretation qualitatively explains most of the γ-ray branchings between members of the negative-parity multiplet, there are several places involving very highly hindered transitions where it runs into difficulties. We take this to mean that small admixtures in the states are very important in determining these transition rates. However, it is instructive to consider specifically one of the more extreme examples—the 1011.9-keV γ (2.9%) from the 1834.1-keV state to the $\frac{11}{2}-$ 821.9-keV state versus the unobserved (<0.5%) 1834.1-keV γ to the $\frac{5}{2}+$ ground state. With an $\frac{11}{2}-$ assignment for the 1834.1-keV state one would not expect to see the 1834.1-keV γ. However, with a $\frac{9}{2}-$ assignment, the arguments are not so clear. Single-particle estimates[35] for the $t_{1/2}$'s of the 1011.9- ($M1$) and 1834.1-keV ($M2$ or $E3$) γ's are 2.4×10^{-14} and 8×10^{-12} or 4×10^{-9} sec, respectively. According to our above description, the missing $M2$ or $E3$ would involve an apparently very simple $\nu d_{3/2}\rightarrow\nu h_{11/2}$ transition (the $M2$ would be l forbidden); there may also be some hindrance from uncoupling and recoupling the states. On the other hand, the observed 1011.9-keV $M1$ γ requires the simultaneous changes $\nu d_{3/2}\rightarrow\nu h_{11/2}$ and $\pi d_{5/2}\rightarrow\pi h_{11/2}$, each of which is doubly l forbidden. However, l forbiddeness loses much of its meaning in multiparticle transitions and would depend on the relative phases of the transforming states; also core polarization in multiparticle states tends to obviate the l selection rules.[46] Still, multiparticle γ decay is formally absolutely forbidden. Although there are known cases where such transitions take place at enhanced rates (e.g., the 63-keV $E1$ γ in Bk^{250} following Es^{254} α decay[47]), they are not common. When such involved rearrangements are compared, clearly the single-particle estimates lose all meaning, and minute admixtures could easily be the deciding factors.

In this multiplet of three-quasiparticle states, we thus have two different and potentially very rewarding sources of information: (1) The enhanced transitions between the various members of the multiplet should give information about the gross features of the states and should allow one to perform calculations on states at several MeV that normally can be done only near the ground state. (2) The very retarded transitions to states not in the multiplet should allow one to determine some of the admixtures in the states and also something more about the structures of many of the lower-lying states.

C. Vibrational States—the Remaining States

The term "quasiparticle" was used advisedly in the previous section, for the simple shell model becomes less and less of a good approximation for states at these energies. Thus, the states and the transition rates will need to be calculated from the occupation-number approach. When this is done, we expect that much more information will also be forthcoming about the remaining states in Pr^{139}, most of which are probably core-coupled vibrational states. At this time it would be especially interesting to know more about the nature of the 828.1- and 851.9-keV states, which receive considerable population from the three-quasiparticle states. Assuming that our interpretation of the latter is correct, the 828.1- and 851.9-keV states would seem to be constructed from the $d_{5/2}$ ground state coupled to a 2+ quadrupole vibration. That they receive so much population could be explained partly by their receiving it in default of other states being available (cf. the γ-ray branching discussion in the previous section) and perhaps partly by the fact that the three-quasiparticle states undoubtedly contain vibrational admixtures. After all, from one viewpoint three-quasiparticle states and single-quasiparticle-plus-core states are only extreme examples of the same thing.

ACKNOWLEDGMENTS

We are indebted to Dr. W. P. Johnson and H. Hilbert for aid in operating the Michigan State University Cyclotron. We thank R. Eppley for discussions about $M4$ isomers and for supplying us with his information on the $N=81$ isomers before publication. We also thank Dr. J. J. Kolata for his assistance and the use of his delayed-coincidence apparatus. Finally, we thank Dr. H. McManus for some very helpful discussions concerning the nature of three-quasiparticle states.

[44] L. M. Beyer, G. Berzins, and W. H. Kelly, Nucl. Phys. **A93**, 436 (1967).

[45] R. B. Frankel, Ph.D. thesis, University of California, Berkeley, Lawrence Radiation Laboratory Report No. UCRL-11871, 1964 (unpublished).

[46] M. Gmitro, J. Hendeković, and J. Sawicki, Phys. Rev. **169**, 983 (1968).

[47] Wm. C. McHarris, F. S. Stephens, F. Asaro, and I. Perlman, Phys. Rev. **144**, 1031 (1966).